# Polymer Chemistry

Accepted Manuscript






ROYAL SOCIETY OF CHEMISTRY

www.rsc.org/polymers

# Aqueous SET-LRP Catalyzed with *"In Situ"* Generated Cu(0) Demonstrates Surface Mediated Activation and Bimolecular Termination

*Shampa R. Samanta,* [a] *Vasiliki Nikolaou,* [b] *Shauni Keller,* [c] *Michael Monteiro,* [d] *Daniela A. Wilson,* [c] *David M. Haddleton,* [b] *and Virgil Percec* [a,] *

[a]Roy & Diana Vagelos Laboratories, Department of Chemistry, University of Pennsylvania, Philadelphia, Pennsylvania 19104-6323, United States

[b]Department of Chemistry, University of Warwick, Gibbet Hill Road, Coventry, CV4 7AL,UK

[c]Radboud University Nijmegen, Institute for Molecules and Materials, Heyendaalseweg 135, Nijmegen, The Netherlands

[d]Australian Institute for Bioengineering and Nanotechnology, University of Queensland, Brisbane QLD 4072, Australia

**ABSTRACTS**

The aqueous SET-LRP catalyzed with "*in situ*" generated Cu(0) of the two amphiphilic monomers 2-hydroxyethyl acrylate (HEA) and oligo(ethylene oxide) methyl ether acrylate (OEOMEA) was investigated at temperatures from -22 to +25 $^{o}$C. The $k_p^{app}$ values of both monomers are higher at 0 $^{o}$C (4.61 min$^{-1}$ for OEOMEA and 2.60 min$^{-1}$ for HEA) than at 25 $^{o}$C (1.60 min$^{-1}$ for OEOMEA and 1.12 min$^{-1}$ for HEA). These unexpected and unprecedented results are explained by the lower Cu(0) particle size obtained by the disproportionation of CuBr at 0 $^{o}$C in $H_2O$. Poly(OEOMEA) obtained by aqueous SET-LRP at 0 $^{o}$C with the unexpectedly high $k_p^{app}$ = 4.61 min$^{-1}$ exhibits 88% chain-end functionality at 100% monomer conversion, while the theoretical value would have to be ~ 0%. This high experimental chain-end functionality was explained by the slow desorption of the hydrophobic backbone containing the propagating radicals of these amphiphilic polymers from the surface of the catalyst due to their strong hydrophobic effect. Polymer radicals adsorbed on the surface of Cu(0) undergo monomer addition and reversible deactivation but do not undergo the bimolecular termination that requires desorption. This amplified adsorption-desorption process that mediates both

*Correspondence to V. Percec (Email: percec@sas.upenn.edu)

the activation and the bimolecular termination explains the unexpectedly high chain-end functionality of the polymers synthesized by SET-LRP.

## INTRODUCTION

Aqueous Single Electron Transfer-Living Radical Polymerization (SET-LRP) catalyzed with Cu(0) and with "*in situ*" generated Cu(0) was discovered as the first LRP for vinyl chloride,[1,2] although activation with Cu(0) of models of growing species of poly(vinyl chloride) was reported earlier.[3] Subsequently, SET-LRP was expanded to acrylates,[4-17] methacrylates,[8,18-25] acrylamides,[26-31] methacrylamide,[32] acrylonitrile,[33,34] and monomers containing more complex water soluble side groups, such as sugars,[35,36] N-(2-hydroxypropyl) methacrylamide,[32] dimethylacrylamide,[26] N-isopropylacrylamide,[26,37-39] oligo(ethylene oxide) methyl ether acrylate,[40] oligo(ethylene oxide) methyl ether methacrylate,[41] hydroxyethyl acrylate,[10] hydroxyethyl methacrylate[23] and acryloyl morpholine.[42]

At the same time as these developments, the list of solvents used in SET-LRP was expanded to other solvents that in combination with aliphatic *N*-donor ligands, such as tris[(2-dimethylaminoethyl)] amine ($Me_6$-TREN)[4,43-45] and tris(2-amino)ethyl amine (TREN)[1,2,4,16,43-45] mediate the disproportionation of Cu(I)X into Cu(II)$X_2$ and Cu(0).[46] This list includes but is not limited to $H_2O$,[10,26,32,38,40,47] DMSO,[6,7,12,21,23,40,48-51] dimethyl formamide (DMF),[46,47] dimethyl acetamide (DMAC),[46,47] alcohols,[22,48] fluorinated alcohols,[52-54] ethylene carbonate,[46,47] propylene carbonate,[46,47] and different mixtures of solvents with water,[46,47,55] mixtures of two solvents,[46,55] and even blood serum.[56] Most monomers used in SET-LRP can often mediate this disproportionation but do not always dissolve Cu(II)$X_2$ limiting its usefulness under certain conditions.[10,46,57]

The catalyst most frequently employed in SET-LRP is Cu(0) in the form of powder[2,4,12,58] including powder generated by the disproportionation of Cu(I)X in a large diversity of solvents,[12] wire,[12,64,69] activated wire[59-62] and tubes.[63,64] Almost all initiators employed in other metal catalyzed LRP such as

alkyl halides,[65,66] sulfonyl halides,[33,48,65,67-69] N-halides[2,70] can be used as such or modified to become soluble for SET-LRP in various media including $H_2O$. Only very few systematic investigations on SET-LRP with Cu(0) generated by disproportionation of Cu(I)X "*in situ*" in water[26,37,38,42] and in mixtures of water with other solvents are available.[1,2,26,37,38,47]

It is important to mention that from many LRP methods that provide polymers with narrow molecular weight distribution, only SET-LRP generates polymers with both narrow molecular weight distribution and quantitative or near quantitative chain-end functionality.[6,7,48-51,57,71-77] Narrow molecular weight distribution is an important feature of the polymers prepared by LRP but the most significant structural parameter of these polymers is the quantitative or near quantitative chain-end functionality combined with narrow molecular weight distribution. Chain-end functionality is the major parameter of a polymer that allows the construction of complex architectures such as multiple block copolymers,[64,73,76-79] and dendrimers by iterative synthesis.[77-81]

In a previous publication from our laboratory it was reported that the Cu(0) mediated SET-LRP of 2-hydroxyethyl acrylate (HEA) in $H_2O$ and in mixtures of protic solvents with $H_2O$ produces a gel of poly(HEA) (PHEA) exclusively on the surface of the catalysts.[10] Gel formation was not observed when SET-LRP of HEA was performed in MeOH, DMSO or in MeOH containing less than 70% $H_2O$.[10] A fast adsorption to the surface and slow desorption of the hydrophilic chain of PHEA from the surface of the Cu(0) wire catalyst together with the amphiphilic character of PHEA was assumed to be responsible for this process.[10] Therefore, we consider that SET-LRP of hydrophilic monomers containing hydrophobic backbones, amphiphilic monomers, such as HEA,[10] oligo(ethylene oxide) methyl ether acrylate (OEOMEA),[40] oligo(ethylene oxide) methyl ether methacrylate[41], 2-hydroxyethyl methacrylate,[23] N-(2-hydroxypropyl)methacrylamide[32], and acryloyl morpholine[42] exhibit amplified adsorption and desorption processes that may complement the previous studies on the elucidation of the role of the surface of Cu(0) catalyst on the activation and deactivation steps of SET-LRP.[11,58-61] This publication reports the aqueous SET-LRP of HEA and OEOMEA mediated by

"*in situ*" generated Cu(0) catalyst.[26,37,38] The study reported here demonstrates that the surface of Cu(0) is responsible both for the activation of the initiator and dormant growing species, as well as for the much lower extent of bimolecular termination observed during polymer synthesis by SET-LRP.

## RESULTS AND DISCUSSION

### Temperature Dependence of the Aqueous SET-LRP of OEOMEA and HEA Catalyzed by "*In Situ*" Generated Cu(0)

Aqueous SET-LRP of the water soluble monomers OEOMEA and HEA was initiated with the water-soluble initiator oligo(ethylene glycol) methyl ether 2-bromoisobutyrate, OEOMEBr with $M_n$ = 495, and catalyzed by the "*in situ*" generated Cu(0) (**Scheme 1**).

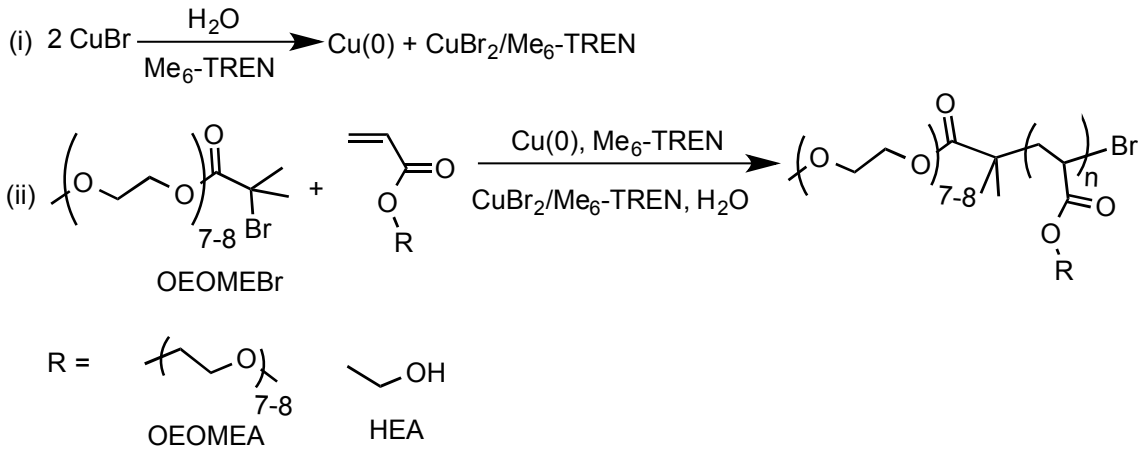


**Scheme 1.** Aqueous SET-LRP of OEOMEA and HEA using OEOMEBr as initiator and catalyzed with "*in situ*" generated Cu(0) obtained from the disproportionation of CuBr in water in the presence of $Me_6$-TREN. (i) disproportionation of CuBr/$Me_6$-TREN in water to form Cu(0) in the absence of monomers and initiator; (ii) addition of monomer and initiator to result in living polymerization.

The preparation of the Cu(0) catalyst by the disproportionation of the CuBr "*in situ*" and the polymerization methodologies follow previously reported procedures elaborated in Percec and Haddleton laboratories (**Figure 1**).[26,37,38] Typically, the required amount of CuBr was added to a deoxygenated solution of $H_2O$ containing an equivalent amount of $Me_6$-TREN to CuBr under $N_2$, and

the solution stirred (stirring rate = 480 rpm) for 30 min to allow complete disproportionation into a 1/1 mixture of Cu(0) and $CuBr_2$. The $K_{eq}$ for the disproportionation of Cu(I)X in water is in the range of $10^6$ to$10^7$.[43,82-88] However, the disproportionation of the crystalline CuBr in the presence of $Me_6$-TREN in water can be limited by a low rate of dissolution in water and therefore, when CuBr is added to water without strong stirring or vortexing, the white crystalline CuBr dissolves at a very low rate, which must represent the rate limiting step of the disproportionation process. Once in solution, CuBr disproportionates rapidly to produce Cu(0) and a blue-green $CuBr_2/Me_6$-TREN solution (**Figure 1**). In this study (see Experimental Section for details), complete disproportionation of CuBr occurs after 5 min stirring of CuBr in $H_2O$ containing $Me_6$-TREN. However, disproportionation for 30 min was carried out to rule out the presence of any trace amount of insoluble CuBr in the solution. To this solution, a deoxygenated mixture of monomer and initiator was injected to the bottom of the reaction mixture *via* a deoxygenated syringe equipped with a long needle. The polymerization started immediately and the monomer conversion was determined by 500 MHz $^1$H NMR spectroscopy at different reaction times.

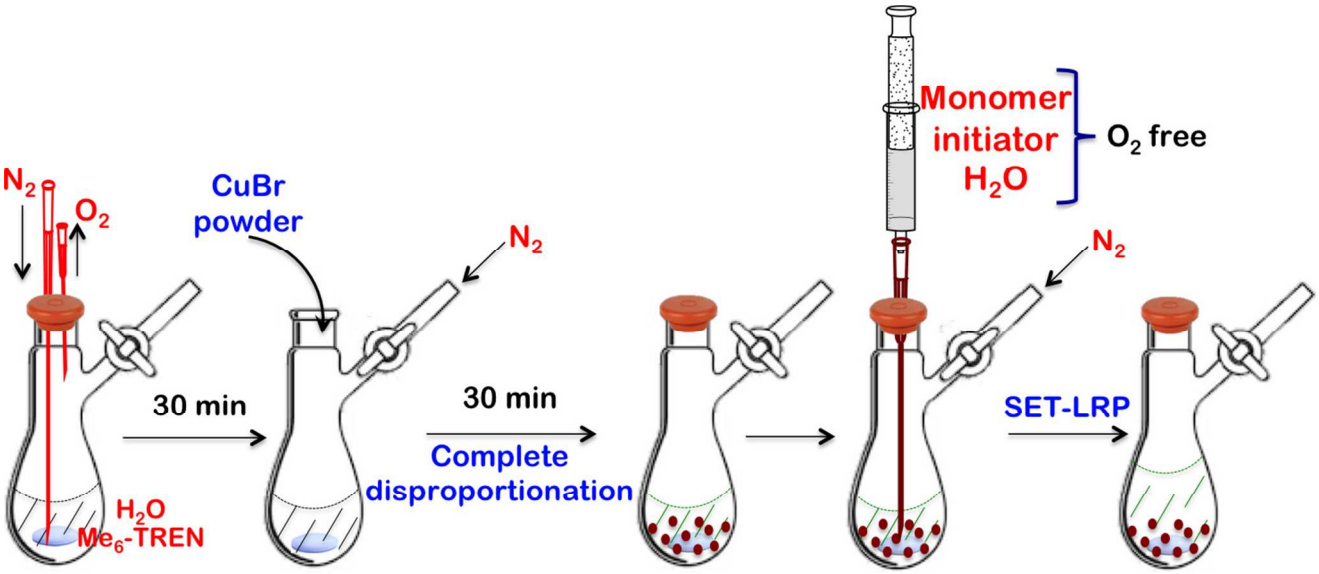


**Figure 1.** Schematic representation of the aqueous SET-LRP catalyzed with Cu(0) generated "*in situ*".

In the polymerization experiments performed at 0, 13 and 25 $^oC$, both the disproportionation and the polymerization were carried out with the reaction mixture equilibrated at the specified

temperature. Experiments at 0 and 13 $^{o}$C were carried out by using ice-water and *p*-xylene/dry-ice bath, respectively. For polymerization targeted at 0 $^{o}$C the thermostat reading was between 0 and 1 $^{o}$C and the reaction mixture was in liquid state. Unexpectedly, $k_p^{app}$ values obtained from the kinetic plots for OEOMEA at 0, 13 and 25 $^{o}$C (**Figure 2**) and for HEA at 0 and 25 $^{o}$C (**Figure 4**) at $[monomer]_0/[I]_0/[CuBr]_0/[Me_6\text{-TREN}]_0$ = 20/1/0.4/0.4 decrease with increasing polymerization temperature. These reactions at 0 $^{o}$C (**Figure 2a, b**), 13 $^{o}$C (**Figure 2c, d**) and 25 $^{o}$C (**Figure 2e, f**) exhibited first order rates of polymerization with respect to monomer concentration, a linear dependence of the number average molecular weight ($M_n$) versus conversion, or theoretical molar mass, and narrow molecular weight distributions (**Figure 3**).

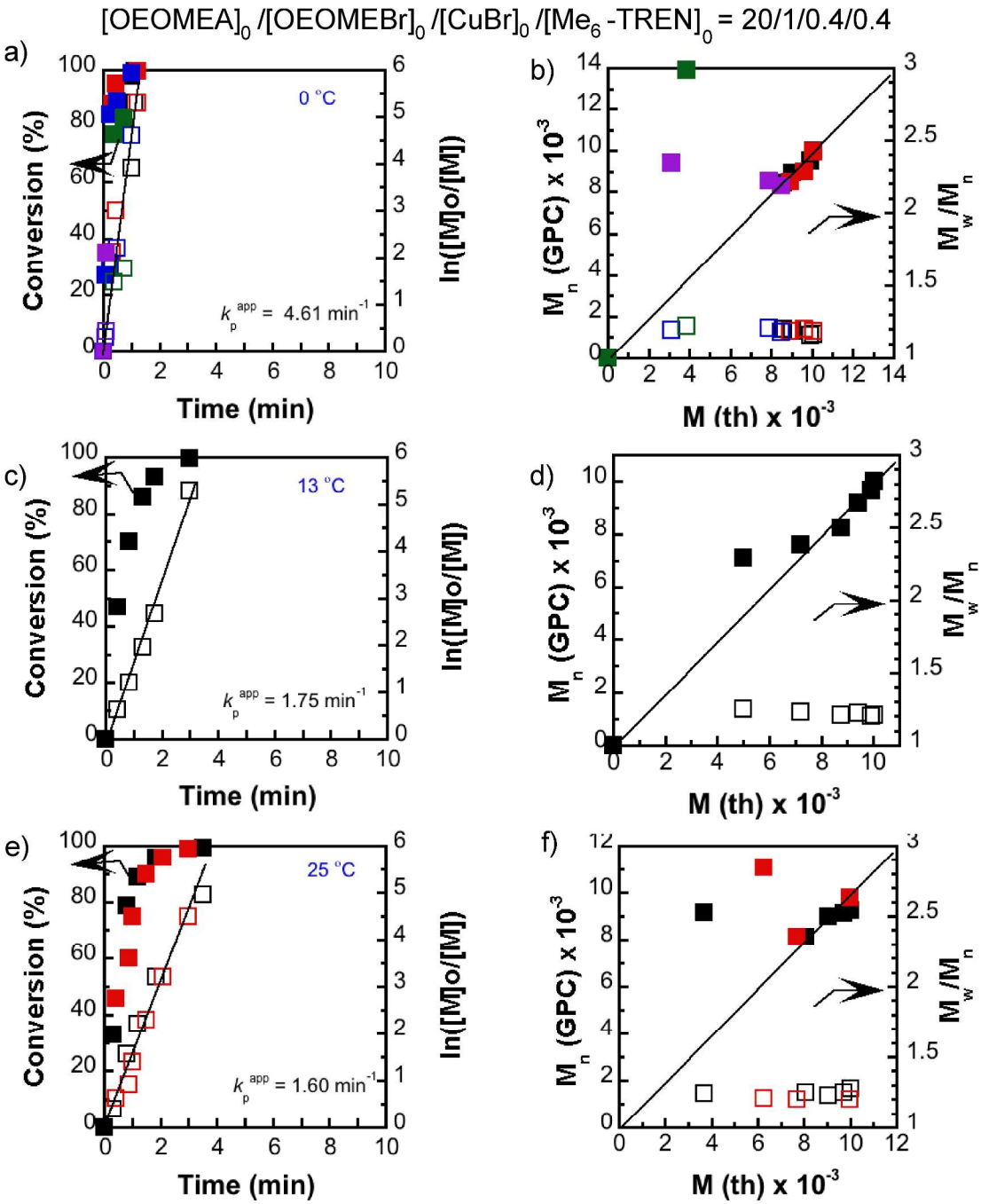


**Figure 2.** Kinetic plots (left) and $M_n$ and $M_w/M_n$ *vs* theoretical $M_{th}$ (right) for aqueous SET-LRP of OEOMEA catalyzed by "*in situ*" generated Cu(0) at 0 °C (a and b), 13 °C (c and d) and 25°C (e and f). Reaction conditions: $[OEOMEA]_0/[I]_0/[CuBr]_0/[Me_6\text{-}TREN]_0$ = 20/1/0.4/0.4, [monomer] = 1.8 M. Experimental data in different colors were obtained from different kinetic experiments.

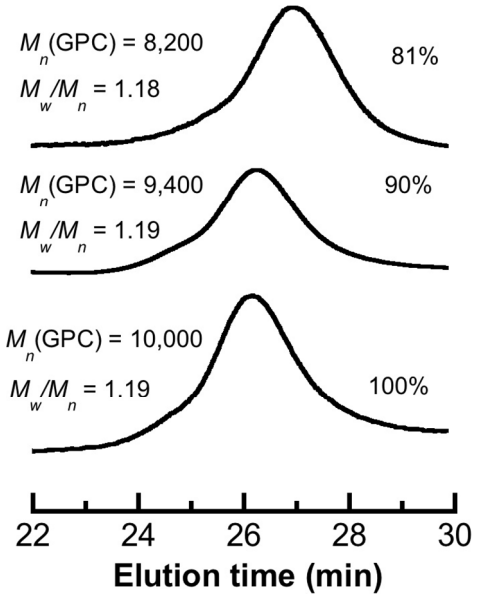


**Figure 3.** GPC traces of poly(OEOMEA) obtained at various monomer conversions of aqueous SET-LRP of OEOMEA catalyzed by "*in situ*" generated Cu(0) at 0 °C . Reaction conditions: $[OEOMEA]_0/[I]_0/[CuBr]_0/[Me_6\text{-TREN}]_0$ = 20/1/0.4/0.4, [monomer] = 1.8 M.

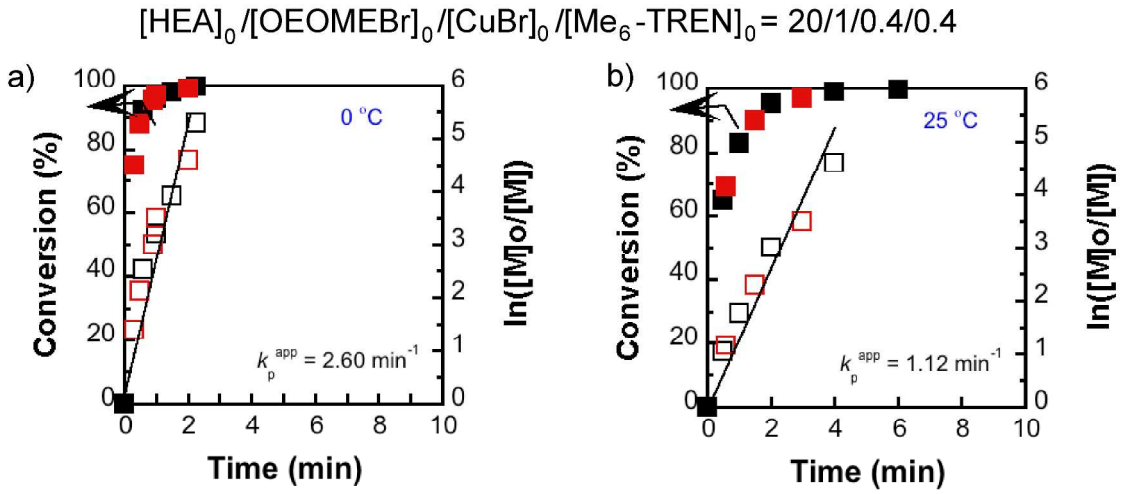


**Figure 4.** Kinetic plots for aqueous SET-LRP of HEA catalyzed by "*in situ*" generated Cu(0) at 0 °C (a) and 25 °C (b). Reaction conditions: $[HEA]_0/[I]_0/[CuBr]_0/[Me_6\text{-TREN}]_0$ = 20/1/0.4/0.4, [monomer] = 1.8 M. Experimental data in different colors were obtained from different kinetic experiments.

A qualitative analysis of the Cu(0) particle size obtained during the disproportionation of $CuBr/Me_6$-TREN revealed much smaller dimensions at 0 °C (**Figure 5a**) than at 25 °C (**Figure 5b**). For the disproportionation at 0 °C the measured temperature was between 0 and 1 °C and the reaction mixture was a liquid. Unexpectedly, at 0 °C water appeared to stabilize the Cu(0) as a stable suspension in a similar way as DMSO does over a large temperature range[43,46] and therefore, a

retardation of the nucleation and growth processes of atomic Cu(0) generated "*in situ*" was observed. In DMSO the colloidal Cu(0) particles exhibit an absorption at $\lambda \sim 600$ nm along with a scattering effect.[43,46,89] Similarly, UV-visible spectra of the colloidal Cu(0) generated in $H_2O$ "*in situ*" by disproportionation of CuBr at 0 $^oC$ exhibited a weak and broad absorption between 375 and 550 nm (**Figure 6a**) due to the absorption and scattering by fine Cu(0) particles. For the disproportionation in $H_2O$ at 0 $^oC$ the Cu(0) particles do not settle completely even 5 min after stirring was interrupted (**Figure 6a**).[43,46,89] As a result, the absorption spectra at 0 $^oC$ (**Figure 6a** ) could not be normalized to zero at any wavelength. Conversely, in the absorption spectra for the disproportionation of CuBr in $H_2O$ at 25 $^oC$ no such effect of Cu(0) was observed and the absorption at 500 nm could be normalized to zero (**Figure 6b**). The degree of disproportionation of CuBr in $H_2O$ for both 0 and 25 $^oC$ were estimated by taking the absorbance of $CuBr_2$ to be the height of the peak at 700 nm and the baseline as the absorbance at 400 nm which is almost a flat region in the case of absorption spectra at 0 $^oC$.[43] It should be noted that, at both temperatures, 100% (± 4%) disproportionation of CuBr into Cu(0) and $CuBr_2$ was observed by UV-visible spectroscopy, by comparing the absorbance of the disproportionated mixture with that of the control solution containing the expected concentration of $CuBr_2$/$Me_6$-TREN solution in $H_2O$ (**Figure 5**). A more detailed investigation of the control of the Cu(0) particle size at various temperatures and their correlation with the $k_p^{app}$ will be reported elsewhere.

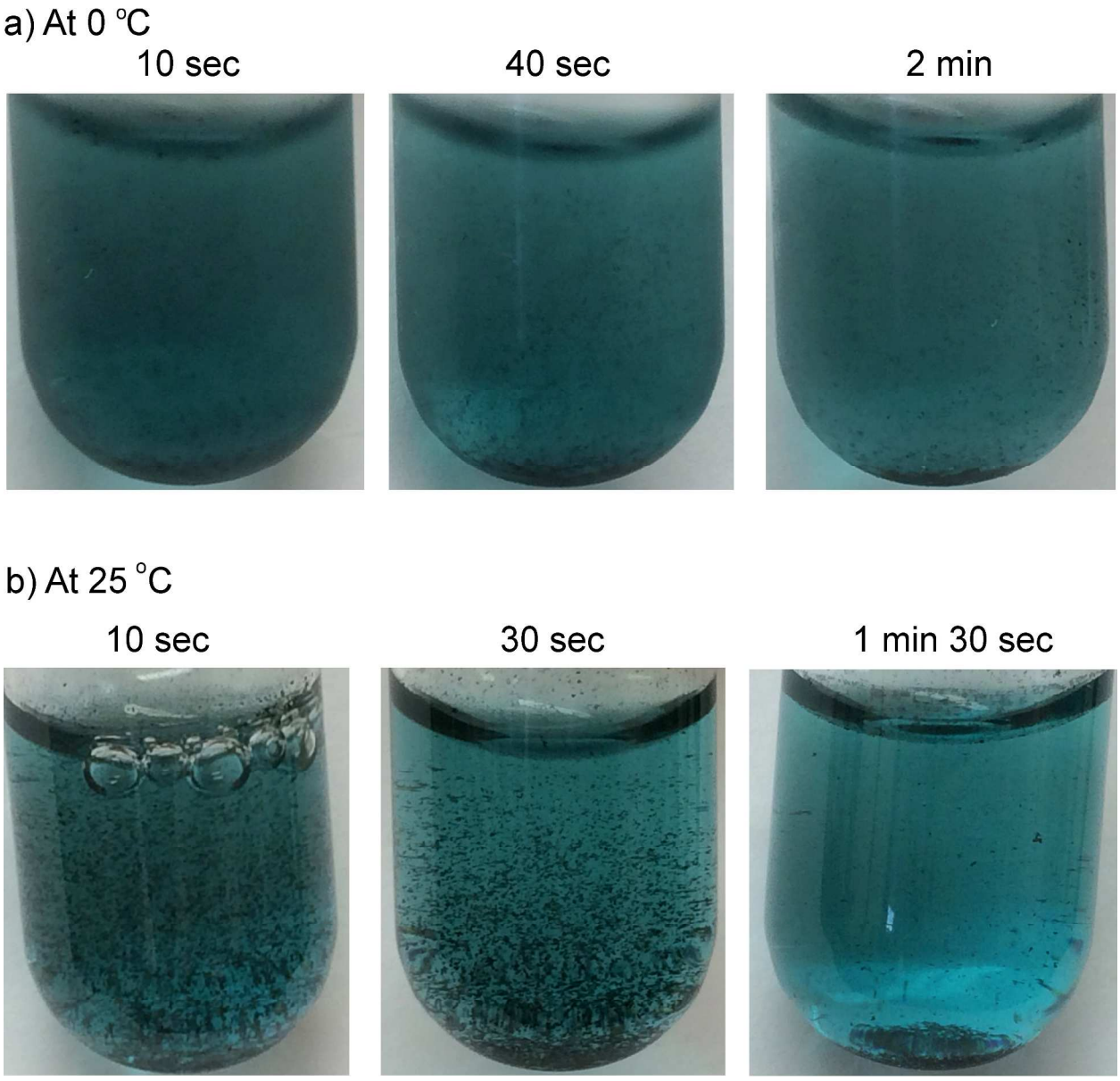


**Figure 5.** Visual observation of the disproportionation of $[CuBr]_0/[Me_6\text{-TREN}]_0$ =1/1 at (a) 0 °C, and (b) 25 °C at different time intervals after stirring of the solution (for 5 min) was stopped. Conditions: $H_2O$ = 1.8 mL, [CuBr] = 15.2 mM, $[CuBr]/[Me_6\text{-TREN}]$ = 1/1.

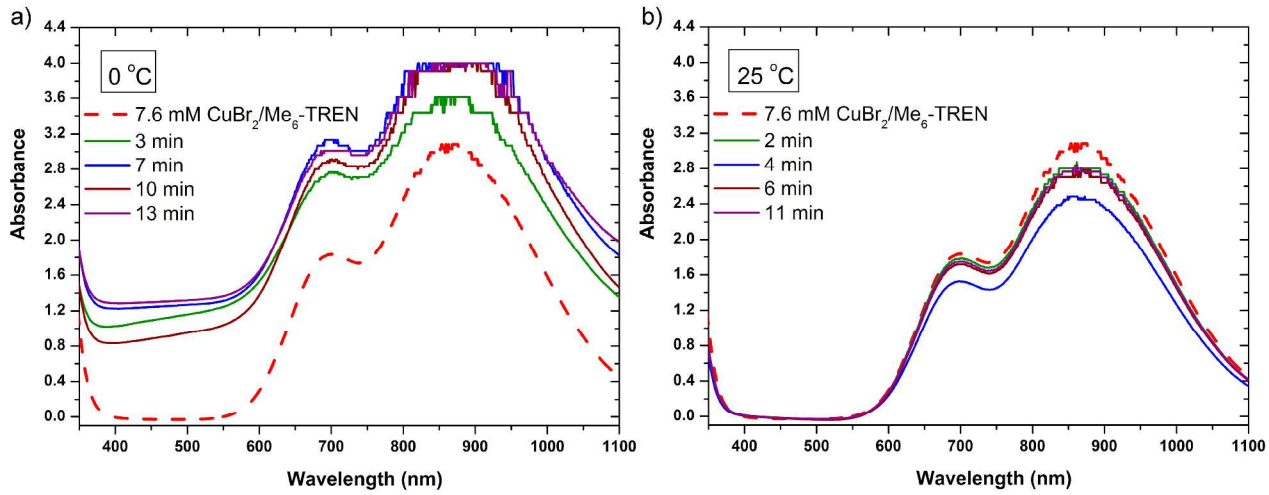


**Figure 6.** UV-vis spectra of the disproportionation of CuBr/$Me_6$-TREN in $H_2O$ at 0 °C (without normalization) (a), and at 25 °C (after normalization) (b) after different time. The dashed line represents the absorption spectrum of the expected CuBr/$Me_6$-TREN (1/1) solution if 100% disproportionation is achieved. Conditions: $H_2O$ = 1.8 mL, [CuBr] = 15.2 mM, [CuBr]/[$Me_6$-TREN] = 1/1, stirring rate = 480 rpm.

The aqueous SET-LRP catalyzed with "*in situ*" generated Cu(0) of OEOMEA was also carried out at -10 and -22 °C (**Figure 7**). In these experiments the disproportionation of CuBr was carried out at 0 °C to prevent the freezing of the disproportionation mixture. The mixture of monomer and initiator was cooled to the polymerization temperature added to the flask containing Cu(0) and $CuBr_2$/$Me_6$-TREN obtained by disproportionation at 0 °C, and immediately immersed into the bath cooled at polymerization temperature. However, unlike the previous trend observed where $k_p^{app}$ increased by lowering the temperature from 25 to 0 °C (**Figure 2 and 3**), the $k_p^{app}$ obtained at -22 and -10 °C were lower than the value obtained at 0 °C (**Figure 6**). This is as under these conditions the reaction mixtures were in a frozen state throughout the polymerization. It is remarkable that even at such a low temperature and under heterogeneous reaction condition $k_p^{app}$ values as high as 0.09 $min^{-1}$ and 0.38 $min^{-1}$ were obtained at – 22 °C and -10 °C, respectively. This demonstrates that "*in situ*" generated Cu(0) is an extremely reactive catalyst for the activation of alkyl halides.

It should be noted that the extremely high catalytic activity of Cu(0) atoms was demonstrated as early as 1968 by P. L. Timms through the reductive dehalogenation reaction of volatile boron-

chlorine compounds by Cu(0) atoms, condensed together on a liquid nitrogen-cooled surface (-196 $^{o}$C).[90] Followed by this experiment, the dehalogenation of ethyl bromide at -196 $^{o}$C by Cu(0) atoms to give the coupling product butane as well as the disproportion product was also reported by the same laboratory.[91] In a further report from the Chanon laboratory the reaction of substituted bromobenzene with Cu(0) atoms at -108 $^{o}$C was shown to generate substituted phenyl radicals and a SET mediated catalysis mechanism by Cu(0) to generate phenyl radicals was proposed.[92] In addition to these studies with atomic Cu(0), a vast amount of evidences for the high catalytic activity of Cu(0) atoms was reported for Ullmann reaction and polymerization on the surface of Cu(0). For instance, a critical analysis of the Ullmann reaction on Cu(111) surface was reported in 2011 by the Wang laboratory (**Scheme 2**).[93] In this study, the intermediates involved were visualized at single-molecule resolution by STM. The authors demonstrated that although the activation of alkyl halides takes place at temperatures as low as -98 $^{o}$C, the dissociation of the Cu atom on the surface from the aryl group needs a higher temperature and complete dissociation occurs only when the sample was annealed at 175 $^{o}$C.[93] This demonstrated strong adsorption of organic species on the surface of Cu(0) and supports the similar polymer adsorption experiments reported here. A detailed discussion on the catalysis of Cu(0) for alkyl and aryl halides can be found in a recent review from our laboratory.[94] This report clearly indicates that the activation of alkyl or aryl halides by Cu(0) takes place by consecutive adsorption and desorption steps where desorption is relatively a slow process compared to the activation. In this present report, the effect of a slow desorption process of a growing amphiphilic polymer radical from the Cu(0) surface in aqueous phase has been demonstrated to result in an unexpectedly low bimolecular termination of the propagating radicals.

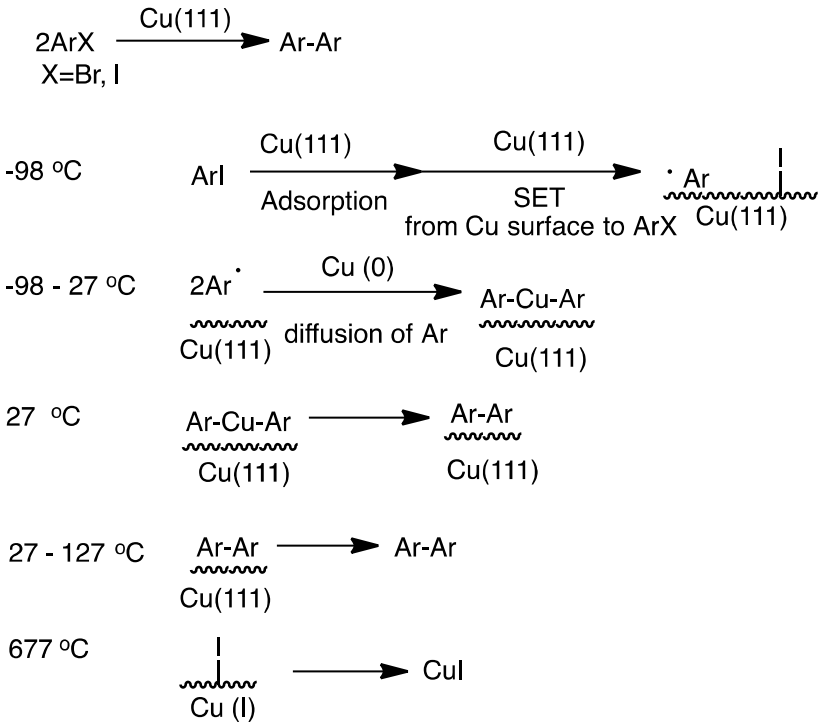


**Scheme 2.** The Mechanism of Ullmann Reaction on the Surface of Cu(0)[93] (adapted from ref [94])

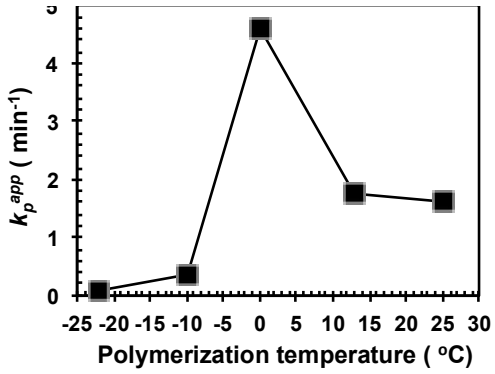


**Figure 7.** The dependence of $k_p^{app}$ on temperature for aqueous SET-LRP of OEOMEA catalyzed with "*in situ*" generated Cu(0). Reaction conditions: $[OEOMEA]_0/[I]_0/[CuBr]_0/[Me_6\text{-TREN}]_0$ = 20/1/0.4/0.4, [OEOMEA] = 1.8 M.

**Analysis of the Chain-End Functionality of Poly(OEOMEA) and PHEA Prepared by Aqueous SET-LRP Catalyzed with Cu(0) Generated "*In Situ*"**

MALDI-TOF experiments were carried out for the analysis of the chain-ends of poly(OEOMEA) with 2-(4-hydroxyphenylazo)benzoic acid as the matrix. However, the signals for ethylene glycol repeat units (60 Daltons) were broad, most probably due to their polydispersity, and

overlapped the signals corresponding to poly(OEOMEA) that lost the bromine chain-end (80 Daltons). On the other hand, the MALDI-TOF spectra of PHEA were reported to give a distorted baseline since PHEA is difficult to ionize due to the requirement of high laser power.[95] In addition, it was also reported that PHEA with bromine end groups undergoes a nucleophilic substitution reaction with the residual $H_2O$ present in the PHEA both in the solution and in gas phase. Therefore, the quantitative analysis of the chain-end of PHEA and poly(OEOMEA) was carried out only by $^1$H NMR spectroscopy.

The chain-end functionality of the poly(OEOMEA) as a function of monomer conversion for the aqueous SET-LRP of OEOMEA catalyzed with Cu(0) generated "*in situ*" at $[OEOMEA]_0/[I]_0/[CuBr]_0/[Me_6\text{-TREN}]_0 = 20/1/0.4/0.4$ at 0 $^oC$ ($k_p^{app} = 4.61$ min$^{-1}$) was determined by thioetherification of the bromine end group with thiophenol *via* the "thio-bromo" click reaction (**Figure 8a**)[7,50,77,78,96] followed by the integration of the ratio of the phenyl ($\delta = 7.45$ □□□ ) and the initiator ($\delta = 1.15$ □□□ ) moiety resonances of the resulting polymer (**Figure 8a, b**) by 500 MHz $^1$H NMR spectroscopy.[6,7,9,48-51,71-78,96] The chain-end functionality of poly(OEOMEA) was 100% at 34% monomer conversion decreasing to 88% at 100% monomer conversion (**Figure 8b**). The 100% chain-end functionality of poly(OEOMEA) at 34% of monomer conversion is in agreement with the absence of the persistent radical effect (PRE)[97] in SET-LRP.[7,50,77,78,96] The PRE[97] is present in ATRP and other metal catalyzed LRP[97] and is required to generate the excess of $CuBr_2$ deactivator at the initial stages of the polymerization. In the case of PHEA polymerized under the conditions ($[HEA]_0/[I]_0/[CuBr]_0/[Me_6\text{-TREN}]_0 = 20/1/0.4/0.4$ at 0 $^oC$ ($k_p^{app} = 2.60$ min$^{-1}$), the chain-end functionality of the polymer was 91% at 100% monomer conversion (**Figure 9**).

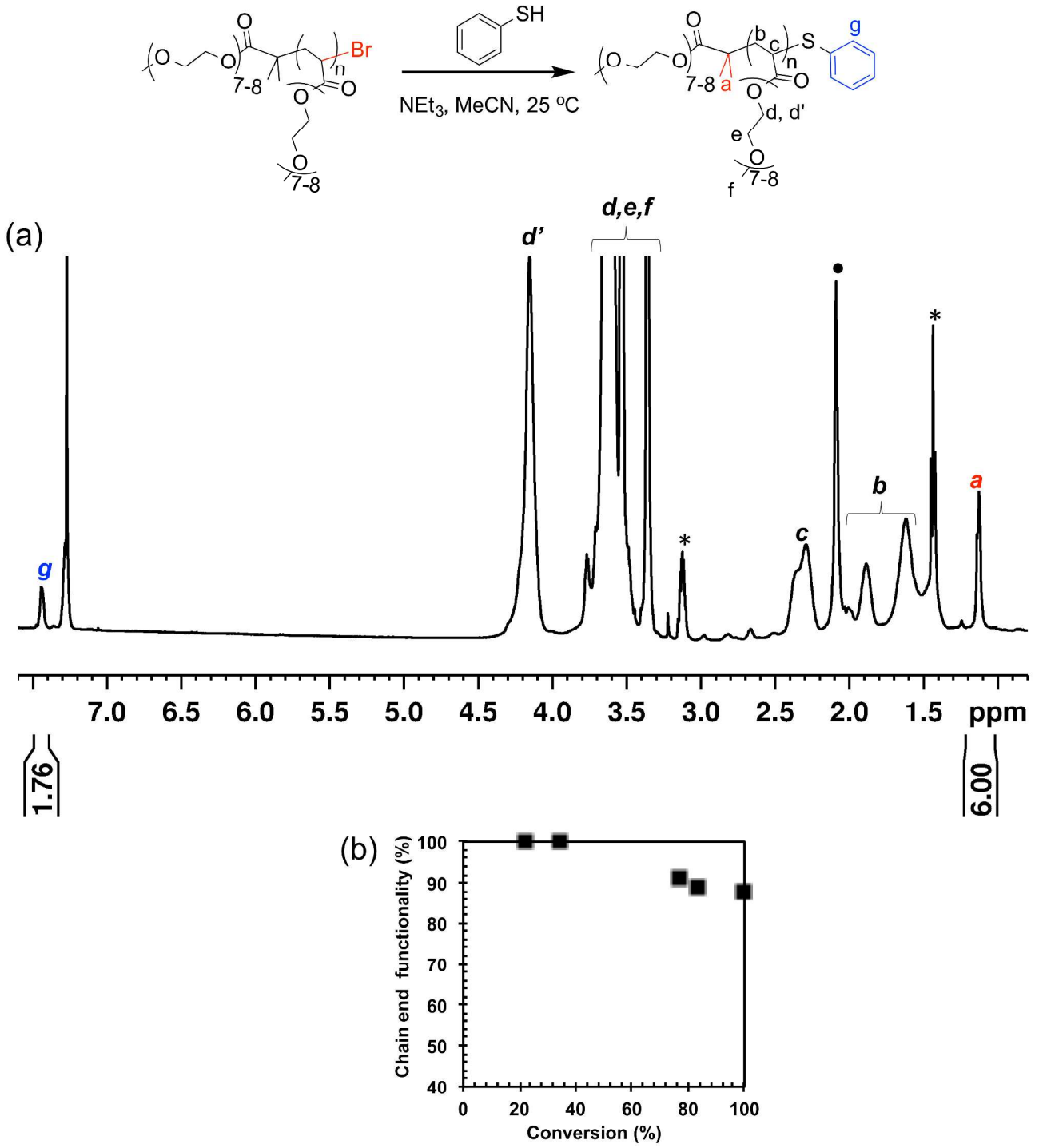


**Figure 8.** $^{1}$H NMR spectrum recorded in $CDCl_3$ along with the assignment of the various protons after thioetherification of bromine chain-end by "thio-bromo" click reaction[7,50,77,78,96] of poly(OEOMEA) at 100% monomer conversion (a), and evolution of chain-end functionality with conversion (b) for the aqueous SET-LRP of OEOMEA mediated by "*in situ*" generated Cu(0) using OEOMEBr as initiator. Reaction conditions: $[OEOMEA]_0/[I]_0/[CuBr]_0/[Me_6\text{-TREN}]_0$ = 20/1/0.4/0.4, [OEOMEA] = 1.8, M, at 0 °C. $^{1}$H NMR resonances from residual diethyl ether and acetonitrile present with the poly(OEOEMA) is indicated with "*" and "•", respectively.

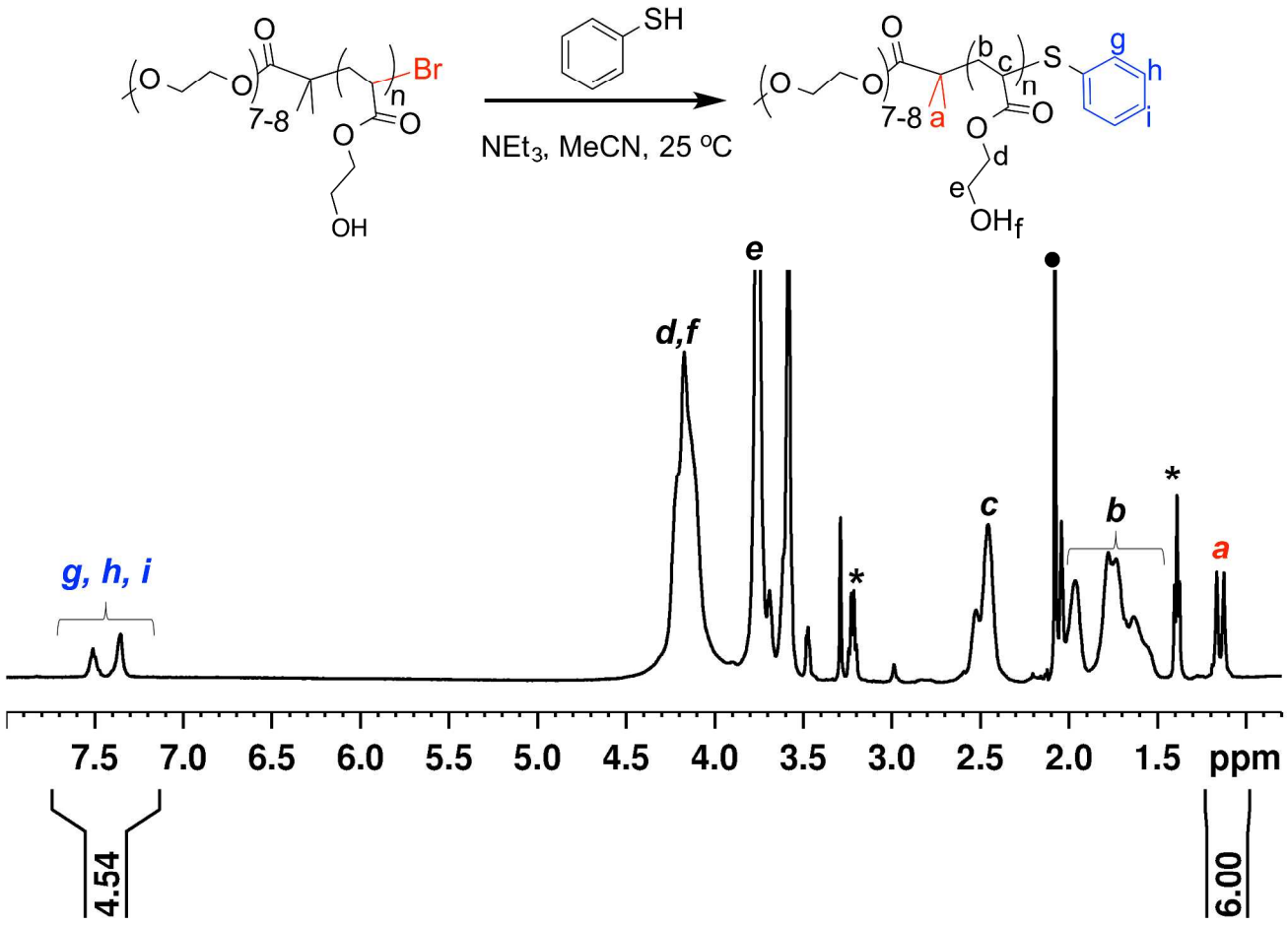


**Figure 9.** $^{1}$H NMR spectrum recorded in acetone-$d_6$ along with the assignment of the various protons after thioetherification of bromine chain-end by "thio-bromo" click reaction[7,50,77,78,96] of PHEA at 100% monomer conversion for the aqueous SET-LRP of HEA mediated by "*in situ*" generated Cu(0) using OEOMEBr as initiator. Reaction conditions: $[HEA]_0/[I]_0/[CuBr]_0/[Me_6\text{-TREN}]_0$ = 20/1/0.4/0.4, [HEA] = 1.8, M, at 0 °C. $^{1}$H NMR resonances from residual diethyl ether and acetone present with the PHEA and acetone-$d_6$ are indicated with "*" and "•", respectively.

The fraction of polymer without Br chain-ends (dead polymer) that is produced by bimolecular termination (eq. 1) during the aqueous SET-LRP of OEOMEA at $[OEOMEA]_0/[I]_0/[CuBr]_0/[Me_6\text{-TREN}]_0$ = 20/1/0.4/0.4 polymerized at 0 °C with $k_p^{app}$ = 4.61 min$^{-1}$ was calculated by the linear regression of eq. 2, where, $k_t$ is the rate constant of bimolecular termination, and [P•] is the concentration of the growing radicals at the time $t$. The value of $k_p$[P•] is constant over the entire polymerization and is demonstrated by its linear first order kinetic (**Figure 3a**). Therefore, it can be assumed that both the $k_p$ and [P•] are constant over the entire polymerization. This means that the concentration of dead polymer, ($[Dead\ polymer]_t$), and the concentration of polymer with active

bromine groups, ([Polymer-Br]$_t$), over the polymerization time can be calculated from eq. 2 and eq. 3.

$$\frac{d[Dead\ polymer]}{dt} = k_t[P\bullet]^2 \qquad Eq.\ 1$$

since [P•] is a constant over time, we get

$$[Dead\ polymer]_t = k_t[P\bullet]^2 t \qquad Eq.\ 2$$

$$[Polymer-Br]_t(\%) = \frac{[I]_0 - [Dead\ polymer]_t}{[I]_0} \times 100 \qquad Eq.\ 3$$

where $t$ = time in seconds, and [Dead polymer]$_t$ is the concentration of the dead polymer at time $t$. $k_p^{app} = k_p[P\bullet] = 4.61\ min^{-1}$ (for aqueous SET-LRP of OEOMEA at 0 $^oC$). Under the given conditions the expected [Polymer-Br]$_t$ in the absence of termination = [I]$_o$ = 0.09 M. To determine [Dead polymer]$_t$, we assume $k_t$ =1 x $10^8$ and series of values for $k_p$ for the estimation of [P•]. In **Figure 10,** [Polymer-Br]$_t$% (eq. 3) is shown assuming the value of $k_p$ ($M^{-1}\ s^{-1}$) = (a) 1 x $10^4$; (b) 3 x $10^4$; (c) 5 x $10^4$.

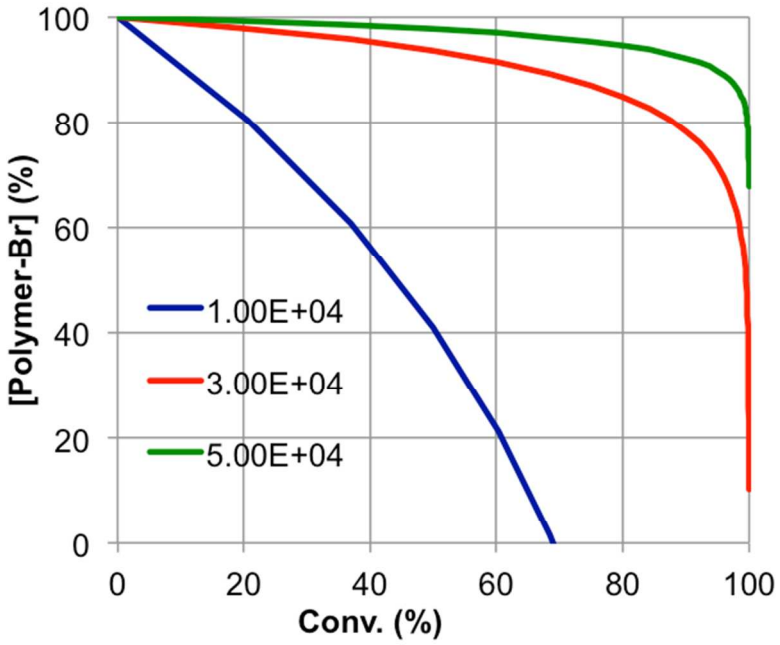


**Figure 10.** Linear regression of eq. 2 to determine the extent of active bromine chain-end functionality [polymer-Br] of poly(OEOMEA) for aqueous SET-LRP of OEOMEA at $k_p^{app}$ = 4.61

$min^{-1}$ mediated by "*in situ*" generated Cu(0), assuming $k_t$ =1 x $10^8$ $M^{-1}$ $s^{-1}$ and of $k_p$ ($M^{-1}$ $s^{-1}$) = (a) 1 x $10^4$; (b) 3 x $10^4$; (c) 5 x $10^4$.

The precise values of $k_p$ and $k_t$ for OEOMEA at 0 °C are not available. Thus, it was assumed that the $k_p = 9.97\times10^3$ $M^{-1}$ $s^{-1}$ of dodecyl acrylate at -3 °C, as obtained by pulsed laser polymerization (PLP), can be used in this case due to the similar chain length of the monomer side groups of OEOMEA and dodecyl acrylate which would take into account monomer diffusion effects.[98] However, the $k_p$ values obtained by PLP shows that they are influenced by several factors,[98] such as monomer concentration and solvent polarity, which in principle should not play a role in the propagation step.[98] Using $k_t = 10^8$ $M^{-1}$ $s^{-1}$ it can be observed that when $k_p$ is set as $10^4$ $M^{-1}$ $s^{-1}$ there is absolutely no chain-end functionality remained at 100% monomer conversion. Only at a $k_p = 5\times10^4$ $M^{-1}$ $s^{-1}$ there is about 68% chain-end functionality left at the complete monomer conversion. As expected, in this case the higher the $k_p$, the higher is the $[\text{Polymer-Br}]_t$ since $k_t$ is assumed to be constant at $10^8$ $M^{-1}$ $s^{-1}$ (**eq. 2** and **3**). Therefore, at $k_p \sim 9.97\times10^3$ $M^{-1}$ $s^{-1}$ for OEOMEA at $[\text{OEOMEA}]_0/[\text{I}]_0/[\text{CuBr}]_0/[\text{Me}_6\text{-TREN}]_0$ = 20/1/0.4/0.4 at 0 °C, for which $k_p^{app}$ = 4.61 $min^{-1}$, instead of 0% chain-end functionality expected from the linear regression of eq. 2, experimental determination of the polymer chain-end functionality. In order to explain such a high extent of chain-end functionality we must consider that the only way to overcome the diffusion controlled bimolecular termination under these reaction conditions is to reduce the concentration of the active radicals in solution. In this instance, the $k_p^{app}$ is extremely high and still the kinetic is first order on [P•], which indicates that a very high [P•] ($7.68\times10^5$ M for $k_p^{app}$ = 4.614 $min^{-1}$, assuming a $k_p$ = $1\times10^4$ $M^{-1}$ $s^{-1}$) is present in the system at any given time. However, it should be noted that during SET-LRP, the activation takes place by a Cu(0) atoms present on the surface of the Cu(0) nanoparticles. This activation method requires the adsorption of the dormant polymer chain on the Cu(0) surface and a SET from the Cu(0) atom to the C-Br moiety of the dormant polymer chain, which is subsequently followed by its desorption from the Cu(0) surface. We hypothesize that during

SET-LRP, the newly generated polymer containing the propagating radical on the Cu(0) surface remains in the adsorbed state while is able to propagate and undergo deactivation by $CuBr_2$, but the diffusion controlled bimolecular termination process is suppressed in its adsorbed state (**Scheme 3**).

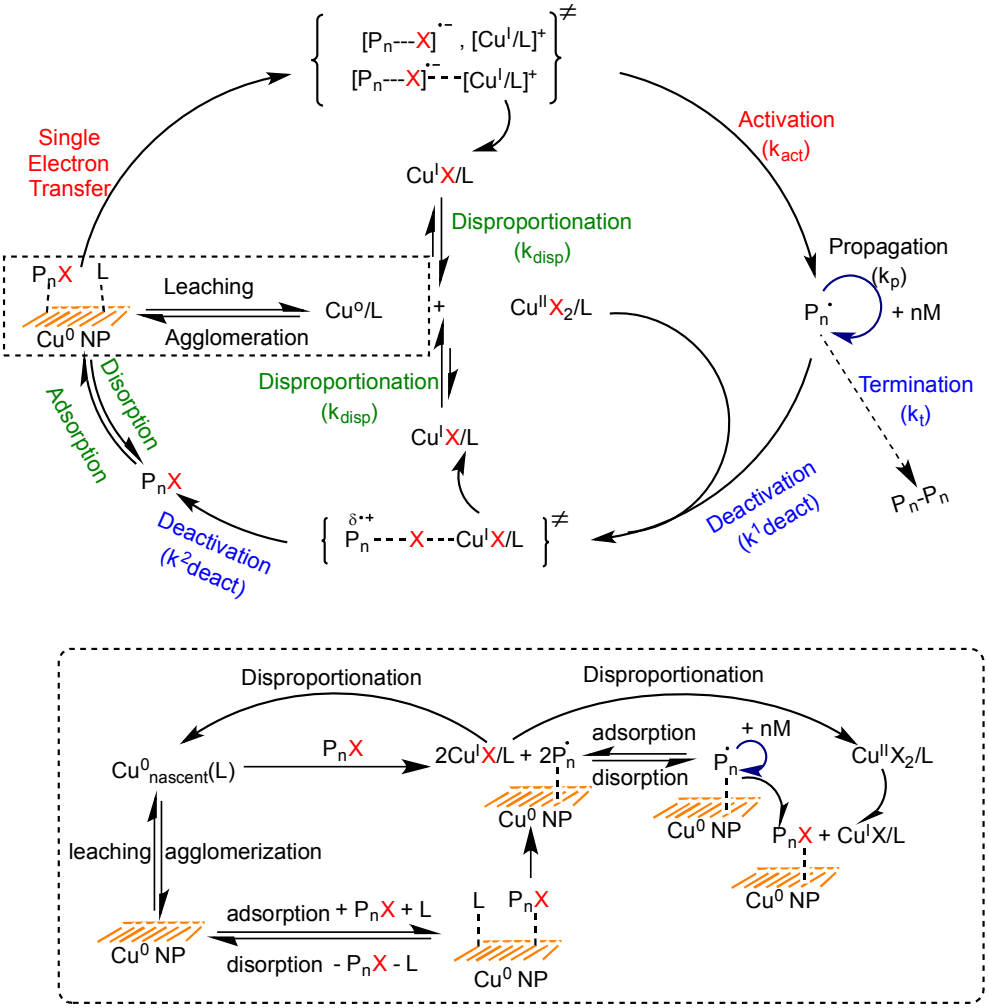


**Scheme 3.** The proposed mechanism for aqueous SET-LRP by "*in situ*" generated Cu(0) nanoparticle obtained by disproportionation of CuBr/$Me_6$-TREN.

It should be noted that SET-LRP is a heterogenous process that proceeds by the Langmuir-Hinshelwood mechanism[9] in which the activation process takes place by SET on the Cu(0) surface.[9,11,58,90-94] Therefore, unlike a homogeneous polymerization, in SET-LRP the adsorption-desorption dynamics of the polymer on Cu(0) surface should greatly influence the diffusion controlled bimolecular termination.[9] SET-LRP in general produces polymers with high chain-end functionality since it does not require PRE[97] like other living radical polymerization techniques. Our laboratory

demonstrated the synthesis of PMA with 100% chain-end functionality by SET-LRP in DMSO with relatively low $k_p^{app}$ values.[6] However, the extent of bimolecular termination continuously increases with the increase of the surface area because of increased $k_p^{app}$ values. For instance, 6% termination was obtained at $k_p^{app}$ ~ 0.01 $min^{-1}$ using 0.5 cm of Cu(0) wire, whereas 13% termination was obtained at $k_p^{app}$ ~ 0.07 $min^{-1}$ using 5.0 cm of Cu(0) wire for SET-LRP of MA targeting DP = 222 in DMSO.[6] Synthesis of PMA by SET-LRP in DMSO does not suppress the bimolecular termination to such a great extent since both PMA and DMSO are polar and adsorption of PMA on the Cu(0) surface is not strongly favored although it takes place. The 88% chain-end functionality of the poly(OEOMEA) prepared by aqueous SET-LRP by "*in situ*" generated Cu(0) at $k_p^{app}$ = 4.61 $min^{-1}$ is expected to be ~ 0% while the experimental value is 88%. This dramatic difference between theoretical and experimental chain-end functionality can be explained by considering an amplified adsorption of amphiphilic polymers containing a hydrophobic backbone and hydrophilic side groups on the hydrophobic surface of Cu(0). Therefore, a longer lifetime of the polymer radical in the adsorbed state reduces the rate of bimolecular termination.

The adsorption-desorption of these polymers in aqueous medium is a dynamic process.[9] Nevertheless, in SET-LRP the activation of alkyl halides *via* SET is dependent on the area of Cu(0) wire[11] or powder,[58] which means both the initiator and the polymer must adsorb on the surface of the catalyst.[9] The fraction of the polymer chain adsorbed on the Cu(0) should be extremely small compared to the total amount of polymer under the LRP condition. This is in agreement with the established Langmuir-Hinshelwood mechanism for activation. [9,90-94]

**Effect of Catalyst and Ligand Concentrations on the Aqueous SET-LRP of OEOMEA Mediated by "*In Situ*" Generated Cu(0)**

Aqueous SET-LRP of OEOMEA at 25 °C with $[monomer]_0/[I]_0/[CuBr]_0/[Me_6\text{-}TREN]_0$ = 20/1/0.4/0.4 yielded $k_p^{app}$ = 1.60 $min^{-1}$. The same polymerization carried out with $[I]_0/[CuBr]_0/[Me_6\text{-}TREN]_0$ = 1/0.8/0.8 and $[I]_0/[CuBr]_0/[Me_6\text{-}TREN]_0$ = 1/1.2/1.2 for OEOMEA generated $k_p^{app}$ = 5.35

min$^{-1}$ and $k_p^{app}$ = 6.31 min$^{-1}$ and a second linear kinetic with lower $k_p^{app}$ after more than 95% conversion (**Figure 11**). For the last two experiments, the chain-end functionality decreased to 73% and 62%, respectively at 99% conversion (**Figure 12**). Under similar reaction conditions at $[I]_0/[CuBr]_0/[Me_6\text{-TREN}]_0$ = 1/0.2/0.2, a linear kinetic with $k_p^{app}$ = 0.42 min$^{-1}$ and 91% polymer chain-end functionality at 100% conversion were obtained (**Figure 12**).

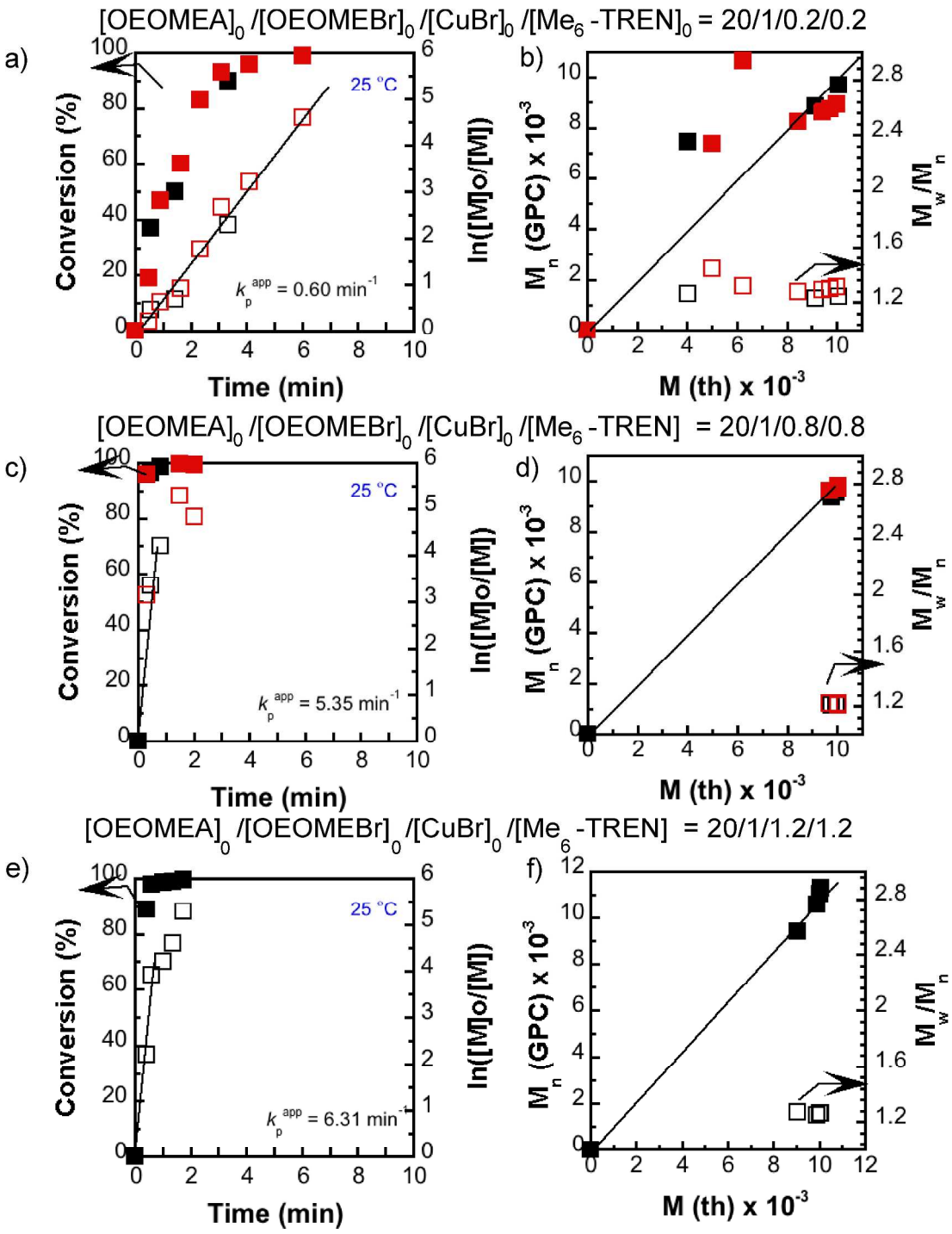

**Figure 11.** Kinetic plots of conversion (%) and ln([M]$_0$/[M]) *vs* time (a, c and e) and experimental $M_n$ and *vs*. theoretical $M_{th,}$ and $M_w/M_n$ (b, d and f) for SET-LRP of OEOMEA in $H_2O$ at 25 $^oC$ for various [I]$_0$/[CuBr]$_0$/[Me$_6$-TREN]$_0$ values. Reaction conditions: [OEOMEA]$_0$/[I]$_0$/[CuBr]$_0$/[Me$_6$-TREN]$_0$ = 20/1/0.2/0.2 (a and b), [OEOMEA]$_0$/[I]$_0$/[CuBr]$_0$/[Me$_6$-TREN]$_0$ = 20/1/0.8/0.8 (c and d), and [OEOMEA]$_0$/[I]$_0$/[CuBr]$_0$/[Me$_6$-TREN]$_0$ = 20/1/1.2/1.2 (e and f). Experimental data in different colors were obtained from different kinetic experiments.

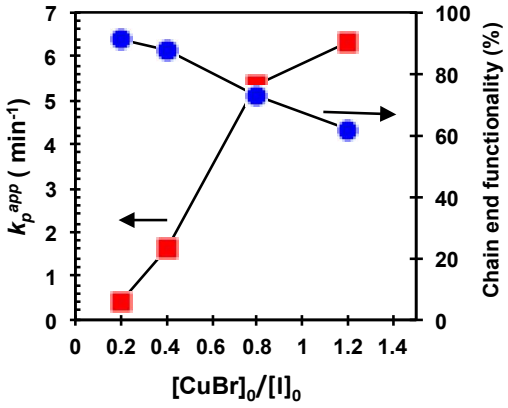


**Figure 12.** Catalyst loading (with respect to [I]$_0$) *vs*. $k_p^{app}$ (red squares) and chain-end functionality (blue spheres) for the aqueous SET-LRP of OEOMEA mediated by "*in situ*" generated Cu(0) obtained by disproportionation of CuBr and initiated by OEOMEBr at 25 $^oC$. Reaction conditions: [OEOMEA]$_0$/[I]$_0$ = 20/1, [CuBr]$_0$/[Me$_6$-TREN]$_0$ = 1/1, [OEOMEA] = 1.8 M.

**Reaction Conditions for Near-Quantitative Chain-End Functionality**

The very fast aqueous SET-LRP of OEOMEA with [OEOMEA]$_0$/[I]$_0$/[CuBr]$_0$/[Me$_6$-TREN]$_0$ = 20/1/0.4/0.4 yielded at 0 $^oC$ $k_p^{app}$ = 4.61 min$^{-1}$ (**Figure 3a**) and an 88% chain-end functionality of the polymer at 100% monomer conversion. Higher chain-end functionality is required for preparative purposes. Therefore, reaction conditions chosen to increase the chain-end functionality with the same concentration of CuBr but different concentrations of ligand were investigated. Under SET-LRP with CuBr/Me$_6$-TREN = 0.4/0.2 a maximum of 55% conversion was obtained after 8 min (**Figure 13 a, b**). SET-LRP with CuBr/Me$_6$-TREN = 0.4/0.3 produced 96% conversion after 6 min with a second linear kinetic regime (**Figure 13 c, d**). Optimum conditions were obtained at CuBr/Me$_6$-TREN = 0.4/0.32 where $k_p^{app}$ =1.93 min$^{-1}$ and a single linear kinetic regime was observed (**Figure 13 e, f**). Poly(OEOMEA) obtained under these conditions has 94% chain-end functionality at 100% monomer conversion.

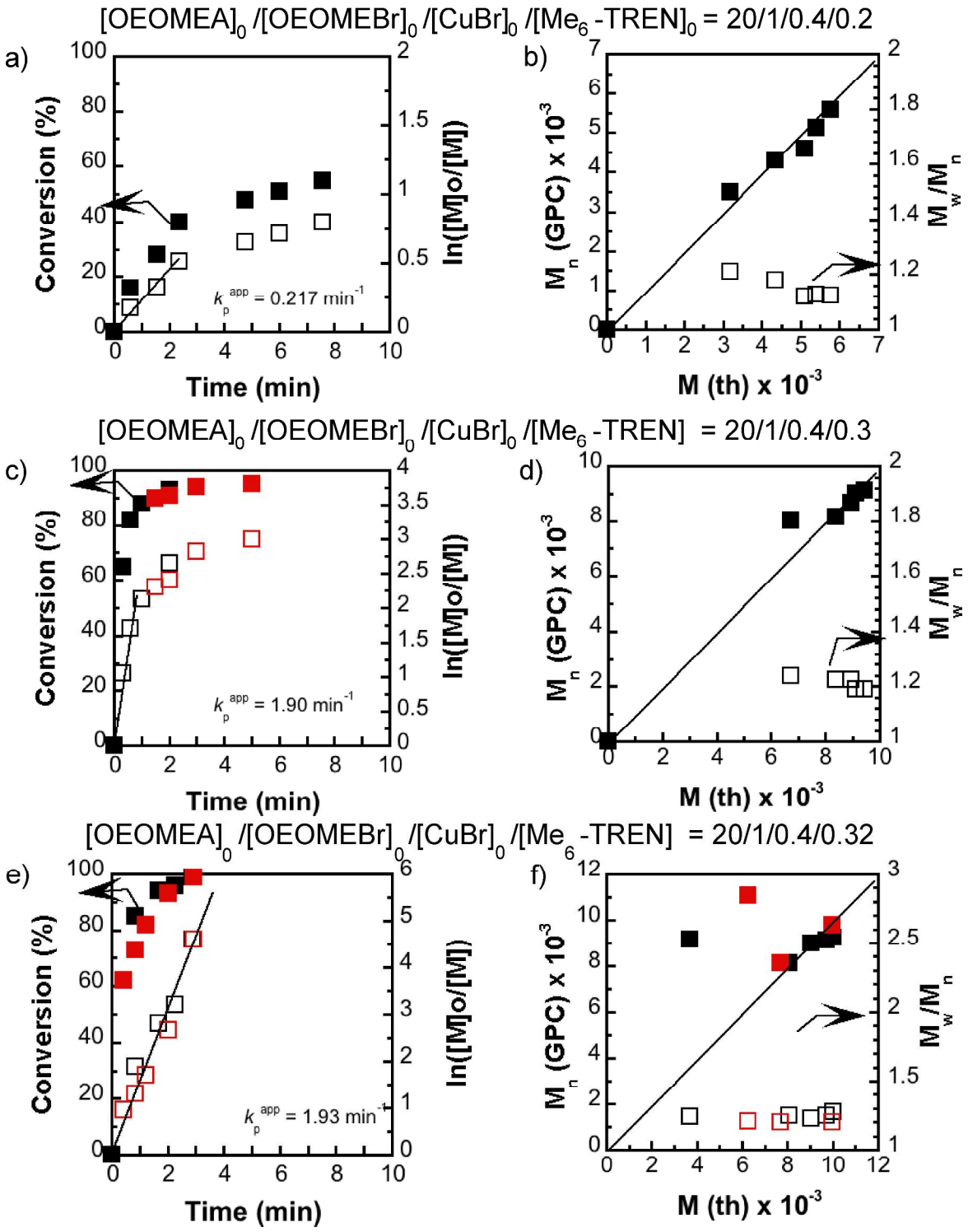


**Figure 13.** Kinetic plots of conversion (%) and ln([M]$_0$/[M]) *vs.* time (a, c and e), and experimental $M_n$ and *vs.* theoretical $M_{th,}$ and $M_w/M_n$ (b, d and f), for SET-LRP of OEOMEA in $H_2O$ at 0 $^oC$ for different concentrations of ligand for [OEOMEA] = 1.8 M, OEOMEA = 1 g, $H_2O$ = 1.1 mL (0.55 mL for the disproportionation experiment and 0.55 mL to the monomer and initiator). Reaction conditions: $[OEOMEA]_0/[I]_0/[CuBr]_0/[Me_6\text{-}TREN]_0$ = 20/1/0.4/0.2 (a and b), $[OEOMEA]_0/[I]_0/[CuBr]_0/[Me_6\text{-}TREN]_0$ = 20/1/0.4/0.3 (c and d), and $[OEOMEA]_0/[I]_0/[CuBr]_0/[Me_6\text{-}TREN]_0$ = 20/1/0.4/0.32 (e and f). Experimental data in different colors were obtained from different kinetic experiments.

**Gel Formation on the Surface of the Catalyst During Aqueous SET-LRP of HEA Catalyzed with Activated Cu(0) Wire**

Aqueous SET-LRP of HEA initiated with OEOMEBr and catalyzed with Cu(0) wire (4.5 cm, 0.812 mm diameter) activated by hydrazine treatment[59] at $[HEA]_0/[I]_0/[Me_6\text{-TREN}]_0$ = 20/1/0.2 in $H_2O$ at 25 $^oC$ produced a thick gel-like PHEA on the surface of the Cu(0) wire (**Figure 14)**. The thickness of the gel increased with monomer conversion. Only a negligible amount of polymer was present in the aqueous phase of the reaction mixture. This gel was insoluble in common organic solvents, indicating that the PHEA was generated by crosslinking of the polymer chains adsorbed on the surface of the Cu(0) wire. The formation of gel-like PHEA was also reported by our laboratory when ethyl α-bromoisobutyrate (EBiB) was used as initiator for aqueous SET-LRP of HEA catalyzed with activated Cu(0) wire.[10] The same gel structure was obtained during SET-LRP of HEA in mixtures of protic solvents and $H_2O$ when the water content was 70 % or higher.[10] In water the hydrophilic side groups of PHEA enhance the hydrophobic effect of the polymer backbone and therefore amplifies its adsorption on hydrophobic surface of the Cu(0) wire catalyst. The strong amphiphilic character of PHEA combined with its amplified hydrophobic effect in water decreases the rate of desorption of PHEA from the surface of the Cu(0) during SET-LRP. Therefore, the lifetime of the propagating radicals adsorbed on the Cu(0) wire surface increases. Their rate of bimolecular termination decreases and therefore they undergo neighboring group or anchimeric[99-104] assisted intramolecular and intermolecular chain transfer reactions that crosslink the polymers from the surface of the Cu(0) wire. The addition of 0.2 equivalents of external deactivator, $CuBr_2$ to the reaction mixture during SET-LRP of HEA using Cu(0) wire as catalyst at $[HEA]_0/[I]_0/[Me_6\text{-TREN}]_0/[CuBr]_2$ = 20/1/0.4/0.2 produced perfectly soluble PHEA with $k_p^{app}$ = 0.17 $min^{-1}$ and linear kinetics up to 99% monomer conversion in 30 min ($M_{th}$ of the acetylated PHEA = 2,836, $M_n$(GPC) = 3,210, $M_w/M_n$ = 1.21). This confirms that the gel formation on the surface of Cu(0) wire in the absence of external $CuBr_2$ is due to the high concentration of polymer radicals that are less reactive for bimolecular termination than for

neighboring repeat units from the surface of Cu(0) wire. SET-LRP of HEA in dipolar aprotic solvents, such as DMSO, MeOH, and mixtures of MeOH with less than 70% water generate soluble PHEA.[10] These solvents and solvent mixtures decrease the hydrophobic effect of the PHEA backbone and therefore increase the desorption rate of the polymer from the surface of the Cu(0) wire.

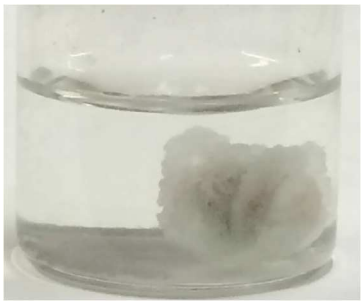

**Figure 14.** (a) Gel formation during aqueous SET-LRP of HEA catalyzed with activated Cu(0) wire. Reaction conditions: HEA = 0.5 mL, $H_2O$ = 1 mL, $[HEA]_0/[I]_0/[Me_6\text{-TREN}]_0$ = 20/1/0.2, hydrazine activated 4.5 cm, 0.812 mm diameter Cu(0) wire, 25 $^oC$.

In water, when Cu(0) wire is used as a catalyst, a large number of amphiphilic polymers with hydrophobic backbones and hydrophilic side groups in their dormant or radical form can be adsorbed on the surface of the catalyst. After SET to the dormant polymers (alkyl halides) from the Cu(0), the local concentration of the polymer radicals on the Cu(0) surface should be much higher compared to a homogeneous reaction medium. The addition of external $CuBr_2$ eliminates the gel formation. This also indicates that at the beginning of the polymerization the concentration of $CuBr_2$ which is generated *via* the disproportionation of CuBr is not sufficient to effectively suppress the large amount of polymer radicals. This is expected, as water is a highly polar solvent and accelerates the SET process that proceeds through a polar transition state.[47] The exact mechanism of gel formation during SET-LRP of HEA by activated Cu(0) wire in the absence of external $CuBr_2$ has not been elucidated and it is outside the scope of this manuscript. However, this crosslinking reaction that was published previously,[10] provided inspiration for the research reported here. We must recall that Cu(0) is a better electron donor than CuX in SET reactions.[9] At the same time $CuX_2$ is both mediating the reversible termination and acts as a SET acceptor and therefore as an oxidant.[9,94] $CuX_2$ as a SET acceptor has

been used as catalyst to create radicals from activated methylenic groups containing CO, COOR, and CN[105-109] and, most probably, also from the ether units of the polymer side groups. This process is well established in the field of radical polymerization[9,94] and in organic chemistry[105-109] (**Figure 15**). More details on the use of $CuX_2$ as catalyst for radical polymerization are available in two comprehensive reviews published in 1982 and 1983.[110,111]

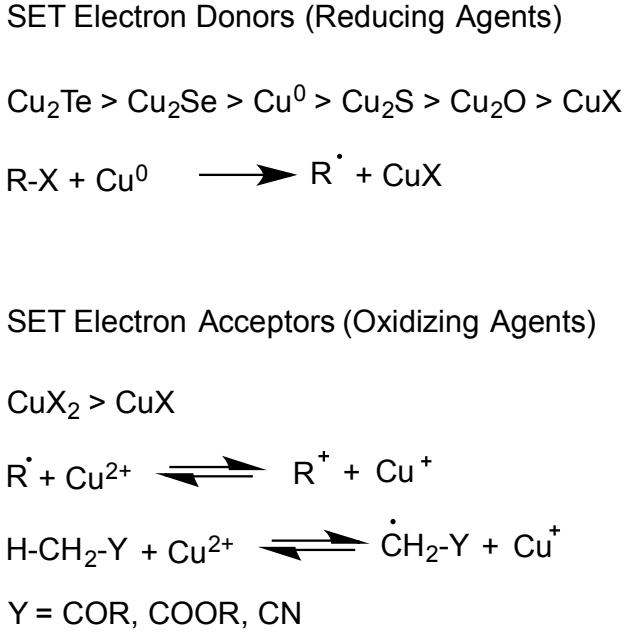


**Figure 15.** Examples of copper oxidizing[9,94] and reducing species [94,105-109] and some of their reactions.

## Conclusions

The aqueous SET-LRP of the two amphiphilic monomers, OEOMEA and HEA catalyzed with "*in situ"* generated Cu(0) was investigated at different temperatures. The $k_p^{app}$ values obtained at low temperatures are higher than those obtained at higher temperatures. This unexpected and unprecedented result was explained by the formation of smaller Cu(0) particles at lower temperatures in water. The simulation of the expected chain-end functionality of poly(OEOMEA) considering $k_p$ = $10^4$ $M^{-1}s^{-1}$ and $k_t$ = $10^8$ $M^{-1}s^{-1}$ for the case of $k_p^{app}$ = 4.61 $min^{-1}$ of OEOMEA revealed that the chain-end functionality at complete monomer conversion should be ~ 0%. Nevertheless, an 88% chain-end functionality of poly(OEOMEA) was experimentally determined at 100% monomer conversion

indicating that during aqueous SET-LRP mediated by "*in situ*" generated Cu(0) the diffusion controlled bimolecular termination process is suppressed. This high chain-end functionality does not take into account the small amount of polymer chain-ends containing –OH groups obtained by anchimerically assisted hydrolysis[112] during SET-LRP.[37] If this concentration would be taken into account, the extent of bimolecular termination observed during aqueous SET-LRP would be even lower. Consequently, we propose that this unexpectedly high chain-end functionality obtained by SET-LRP is the result of the growing polymer radical being adsorbed on the Cu(0) surface since the activation step takes place by Cu(0) atoms from the surface of Cu(0) particles. Hence, both the propagation and reversible deactivation steps proceed while the growing polymer radical is in the adsorbed state on the surface of the catalyst the same adsorbed polymer cannot undergo bimolecular termination before being completely desorbed from the Cu(0) surface. The gel formation around the Cu(0) wire during SET-LRP of HEA in aqueous medium using Cu(0) wire as catalyst is mediated by a neighboring group or anchimeric effect and supports the role of adsorption and desorption steps in the activation and in the reduced extent of bimolecular irreversible termination reported frequently during SET-LRP.[10]

## EXPERIMENTAL

### Materials

Cu wire (20 gauge wire, 0.812 mm diameter from Fischer), HPLC grade water (Fischer) and hydrazine hydrate (100%, hydrazine 64%, Acros) used for the activation of Cu wire were used as received. Oligo(ethylene oxide) methyl ether acrylate (average $M_n$ = 480, Aldrich) was passed through basic alumina to remove the radical inhibitor prior being used in polymerization experiments. OEOMEBr initiator[113] and hexamethylated *tris(*2-aminoethyl)amine ($Me_6$-TREN) [114] were synthesized aby literature procedures. Copper (0) wire (20 gauge wire, 0.812 mm diameter from

Fischer) was activated with hydrazine hydrate according to a procedure elaborated in our laboratory.[59] 2-Hydroxyethyl acrylate (Acros, 97%) was purified following a literature procedure.[10]

**Techniques**

500 MHz $^1$H-NMR spectra were recorded on a Bruker DRX500 NMR instrument at 20 $^o$C in $D_2O$ and $CDCl_3$. Gel Permeation Chromatography (GPC) analysis was performed on a Perkin-Elmer Series 10 high-performance liquid chromatograph, equipped with an LC-100 column oven maintained at 30$^o$C, a Nelson Analytical 900 Series integration data station, a Perkin-Elmer 785 UV-vis detector (254 nm) and two AM gel columns (500 Å, 5 μm; and 1000 Å, 5 μm). HPLC grade THF (Fisher) was used as eluent at a flow rate of 1 mL/min. The number-average molecular weight ($M_n$) and molecular weight distribution ($M_w/M_n$) were determined with poly(methyl methacrylate) (PMMA) standards purchased from American Polymer Standards. PHEA was acetylated by treating with pyridine and acetic anhydride to make it soluble in THF before GPC analysis.[10]

**Typical Procedure for Polymerization Kinetics for Aqueous SET-LRP Catalyzed by "*In Situ*" Generated Cu(0)**

A mixture of $H_2O$ (HPLC, 0.55 mL), and $Me_6$ -TREN (11.25 μL, 0.042 mmol) was added to a 25 mL Schlenk tube fitted with a magnetic stir bar and a rubber septum. The mixture was degassed by purging $N_2$ through the solution for 30 min (rate = 2-3 bubble/s). At the same time the Schlenk tube was immersed in an ice-water bath set at 0 $^o$C for the polymerizations carried out at 0, -10 and -22 $^o$C. For polymerizations performed at 13 and 25 $^o$C the Schlenk tube was immersed in a water bath set at 25 $^o$C and in *p*-xylene/dry-ice bath set at 13 $^o$C. CuBr (5.98 mg, 0.042 mmol) was then carefully added under slight positive pressure of nitrogen. The solution was stirred at 480 rpm for 30 min to generate a bluish green solution of $CuBr_2$/$Me_6$-TREN and the suspension of copper(0) powder. At the same time, to a vial with a magnetic stir bar and a rubber septum, $H_2O$ (0.55 mL), OEOMEBr (51.97

mg, 0.104 mmol) and OEOMEA (1g, 2.083 mmol) were charged and the vial was immersed in the cooling bath set at the polymerization temperature, and fitted and the mixture was bubbled with nitrogen for 30 min. After that, the degassed monomer/initiator solution was transferred *via* a degassed syringe equipped with a long needle through the septum to the bottom of the Schlenk tube with Cu(0)/$CuBr_2$/$Me_6$-TREN. The solution was allowed to polymerize. Samples containing 0.1- 0.2 mL of the reaction solution were then removed for $^1$H NMR and GPC analysis. Catalyst residue was removed by filtration through a column of neutral alumina prior to GPC analysis using THF as eluent. The sample for $^1$H NMR spectroscopy was directly diluted with $D_2O$, and the conversions were determined according to the integral of the vinyl group with that of the -$CH_2$ groups at 3- 3.9 ppm.

**Typical Procedure for Polymerization Kinetics for Aqueous SET-LRP of HEA Catalyzed by Hydrazine Activated Cu(0) Wire**

In a 25-mL Schlenk tube fitted with a rubber septum HEA (0.5 mL, 0.0044 mmol), $Me_6$-TREN (21.75 μL, 0.081 μmol), OEOMEA (91.2 μL, 0.22 μmol), $CuBr_2$ (9.7 mg, 0.043 mmol), and $H_2O$ (1 mL) were added. The reaction mixture was thereafter degassed by purging $N_2$ through the solution for 30 min (rate = 2-3 bubbles/s). After 30 min, hydrazine-activated Cu(0) catalyst (4.5 cm of gauge 20 wire, wrapped around a Teflon-coated stirrer bar) was dropped into the Schlenk tube under positive pressure of $N_2$ and the Schlenk tube was placed in an oil bath thermostated at the desired temperature (25 °C) with stirring. Samples of 0.1- 0.2 mL of the reaction mixture were then removed for $^1$H NMR and GPC analysis. The conversions were determined by $^1$H NMR spectroscopy recorded in $D_2O$. Catalyst residue was removed by filtration through a column of neutral alumina and PHEA was acetylated[10] prior to GPC analysis using THF as eluent.

**Typical Procedure for the Disproportionation of CuBr in $H_2O$ Studied by UV-Vis Spectroscopy**

Disproportionation experiments were performed in 3.5 mL volume Starna UV-Vis quartz cuvettes with airtight screw cap fitting. Photographs were taken with a digital camera using a white background. UV-vis spectra were recorded on a Shimadzu 1601 spectrometer with Shimadzu UV-Probe software. A mixture of deionized water (3 mL) and $Me_6$-TREN (10.46 mg, 0.045 mmol) was taken in the cuvette fitted with a rubber septum and a small stirring bar (5 x 2 mm, Fischer). The cuvette was immersed in a 0 $^oC$ or 25 $^oC$ water bath for the experiments targeted at 0 $^oC$ and 25 $^oC$, respectively. For the experiment at 0 $^oC$ the thermostat reading was between 0-1 $^oC$ and the solution was in liquid state. The solution was purged with $N_2$ for 30 min. Followed, the white crystalline CuBr (6.52 mg, 15.15 mmol) was added carefully to the cuvette under a slightly positive $N_2$ started stirred immediately to generate a bluish green solution of $CuBr_2$/$Me_6$-TREN and the suspension of Copper (0) powder. The stirring was paused at a predefined time to record UV-Vis spectra 1 min after the stirring was interrupted. The stirring was resumed and UV-Vis spectra were recorded repeatedly until the complete disproportionation was obtained.

**Typical Procedure for Chain-End Functionality Analysis of Poly(OEOMEA) and PHEA**

Time required to reach a desired amount of conversion was determined from kinetic experiments under various conditions. A new batch of experiments was carried out for monitoring chain-end functionality. After the polymerization reached desired conversion (typically within 3-6 min), ethyl acetate and $Na_2SO_4$ was added to the solution within a minute. The mixture was stirred for 2 min while $H_2O$ is completely removed by $Na_2SO_4$. The ethyl acetate layer containing polymer was then dried under reduced pressure. The polymer was diluted with ~ 1 mL of acetone and predicated from diethyl ether or diethyl ether/hexane (1/2) mixture to obtain Poly(OEOMEA) and PHEA free of residual $Me_6$-TREN. The polymer was vacuum dried for 12 h. "Thio-bromo" click reaction was carried out by following previously reported method from our laboratory.[50] The thioetherified product was purified once again by precipitation in diethyl ether or diethyl ether/hexane (1/2) mixture from acetone. The $^1H$ NMR was recorded in $CDCl_3$ to determine chain-end functionality.

**Acknowledgements**

Financial support by the National Science Foundation (DMR-1120901, DMR-1066116) and the P. Roy Vagelos Chair at Penn is gratefully acknowledged. S. K. and D. A. W. acknowledge support from the European Research Council under the European Union's Seventh Framework Programme (FP7/2007-20012)/ERC-StG 307679 "StomaMotors" and the Radboud Honors Program at Faculty of Science for the traveling.

**References**

(1) Percec, V.; Popov, A. V.; Ramirez-Castillo, E.; Monteiro, M.; Barboiu, B.; Weichold, O.; Asandei, A. D.; Mitchell, C. M. *J. Am. Chem. Soc.* **2002**, *124*, 4940-4941.

(2) Percec, V.; Popov, A. V.; Ramirez-Castillo, E.; Weichold, O. *J. Polym. Sci., Part A: Polym. Chem.* **2003**, *41*, 3283-3299.

(3) Asandei, A. D.; Percec, V. *J. Polym. Sci., Part A: Polym. Chem.* **2001**, *39*, 3392-3418.

(4) Percec, V.; Guliashvili, T.; Ladislaw, J. S.; Wistrand, A.; Stjerndahl, A.; Sienkowska, M. J.; Monteiro, M. J.; Sahoo, S. *J. Am. Chem. Soc.* **2006**, *128*, 14156-14165.

(5) Zhai, S.; Wang, B.; Feng, C.; Li, Y.; Yang, D.; Hu, J.; Lu, G.; Huang, X. *J. Polym. Sci., Part A: Polym. Chem.* **2010**, *48*, 647-655.

(6) Nguyen, N. H.; Levere, M. E.; Percec, V. *J. Polym. Sci., Part A: Polym. Chem.* **2012**, *50*, 860-873.

(7) Lligadas, G.; Percec, V. *J. Polym. Sci., Part A: Polym. Chem.* **2007**, *45*, 4684-4695.

(8) Coelho, J. F. J.; Silva, A. M. F. P.; Popov, A. V.; Percec, V.; Abreu, M. V.; Gonçalves, P. M. O. F.; Gil, M. H. *J. Polym. Sci., Part A: Polym. Chem.* **2006**, *44*, 2809-2825.

(9) Rosen, B. M.; Percec, V. *Chem. Rev.* **2009**, *109*, 5069-5119.

(10) Leng, X.; Nguyen, N.; van Beusekom, B.; Wilson, D. A.; Percec, V. *Polym. Chem.* **2013**, *4*, 2995-3004.

(11) Nguyen, N. H.; Rosen, B. M.; Lligadas, G.; Percec, V. *Macromolecules* **2009**, *42*, 2379-2386.

(12) Jiang, X.; Rosen, B. M.; Percec, V. *J. Polym. Sci., Part A: Polym. Chem.* **2010**, *48*, 403-409.

(13) Zhai, S.; Shang, J.; Yang, D.; Wang, S.; Hu, J.; Lu, G.; Huang, X. *J. Polym. Sci., Part A: Polym. Chem.* **2012**, *50*, 811-820.

(14) Zhai, S.; Song, X.; Yang, D.; Chen, W.; Hu, J.; Lu, G.; Huang, X. *J. Polym. Sci., Part A: Polym. Chem.* **2011**, *49*, 4055-4064.

(15) Ding, A.; Lu, G.; Guo, H.; Zheng, X.; Huang, X. *J. Polym. Sci., Part A: Polym. Chem.* **2013**, *51*, 1091-1098.

(16) Anastasaki, A.; Waldron, C.; Nikolaou, V.; Wilson, P.; McHale, R.; Smith, T.; Haddleton, D. M. *Polym. Chem.* **2013**, *4*, 4113-4119.

(17) Boyer, C.; Atme, A.; Waldron, C.; Anastasaki, A.; Wilson, P.; Zetterlund, P. B.; Haddleton, D.; Whittaker, M. R. *Polym. Chem.* **2013**, *4*, 106-112.

(18) Chen, G.; Wright, P. M.; Geng, J.; Mantovani, G.; Haddleton, D. M. *Chem. Commun.* **2008**, 1097-1099.

(19) Jones, M. W.; Gibson, M. I.; Mantovani, G.; Haddleton, D. M. *Polym. Chem.* **2011**, *2*, 572-574.

(20) Fleischmann, S.; Percec, V. *J. Polym. Sci., Part A: Polym. Chem.* **2010**, *48*, 4889-4893.

(21) Fleischmann, S.; Percec, V. *J. Polym. Sci., Part A: Polym. Chem.* **2010**, *48*, 2243-2250.

(22) Fleischmann, S.; Percec, V. *J. Polym. Sci., Part A: Polym. Chem.* **2010**, *48*, 2236-2242.

(23) Nguyen, N. H.; Leng, X.; Percec, V. *J. Polym. Sci., Part A: Polym. Chem.* **2013**, *4*, 2760-2766

(24) Song, X.; Zhang, Y.; Yang, D.; Yuan, L.; Hu, J.; Lu, G.; Huang, X. *J. Polym. Sci., Part A: Polym. Chem.* **2011**, *49*, 3328-3337.

(25) Deng, Y.; Li, Y.; Dai, J.; Lang, M.; Huang, X. *J. Polym. Sci., Part A: Polym. Chem.* **2011**, *49*, 4747-4755.

(26) Nguyen, N. H.; Rosen, B. M.; Percec, V. *J. Polym. Sci., Part A: Polym. Chem.* **2010**, *48*, 1752-1763.

(27) Tang, X.; Liang, X.; Yang, Q.; Fan, X.; Shen, Z.; Zhou, Q. *J. Polym. Sci., Part A: Polym. Chem.* **2009**, *47*, 4420-4427.

(28) Deng, Y.; Zhang, J. Z.; Li, Y.; Hu, J.; Yang, D.; Huang, X. *J. Polym. Sci., Part A: Polym. Chem.* **2012**, *50*, 4451-4458.

(29) Feng, C.; Li, Y.; Yang, D.; Li, Y.; Hu, J.; Zhai, S.; Lu, G.; Huang, X. *J. Polym. Sci., Part A: Polym. Chem.* **2010**, *48*, 15-23.

(30) Feng, C.; Shen, Z.; Li, Y.; Gu, L.; Zhang, Y.; Lu, G.; Huang, X. *J. Polym. Sci., Part A: Polym. Chem.* **2009**, *47*, 1811-1824.

(31) Feng, C.; Shen, Z.; Yang, D.; Li, Y.; Hu, J.; Lu, G.; Huang, X. *J. Polym. Sci., Part A: Polym. Chem.* **2009**, *47*, 4346-4357.

(32) Nga Hang, N.; Rodriguez-Emmenegger, C.; Brynda, E.; Sedlakova, Z.; Percec, V. *Polym. Chem.* **2013**, *4*, 2424-2427.

(33) Barboiu, B.; Percec, V. *Macromolecules* **2001**, *34*, 8626-8636.

(34) Liu, X.-H.; Zhang, G.-B.; Li, B.-X.; Bai, Y.-G.; Li, Y.-S. *J. Polym. Sci., Part A: Polym. Chem.* **2010**, *48*, 5439-5445.

(35) Zhang, Q.; Collins, J.; Anastasaki, A.; Wallis, R.; Mitchell, D. A.; Becer, C. R.; Haddleton, D. M. *Angew. Chem., Int. Ed.* **2013**, *52*, 4435-4439.

(36) Zhang, Q.; Wilson, P.; Anastasaki, A.; McHale, R.; Haddleton, D. M. *ACS Macro Lett.* **2014**, *3*, 491-495.

(37) Alsubaie, F.; Anastasaki, A.; Wilson, P.; Haddleton, D. M. *Polym. Chem.* **2015**, *6*, 406-417.

(38) Zhang, Q.; Wilson, P.; Li, Z.; McHale, R.; Godfrey, J.; Anastasaki, A.; Waldron, C.; Haddleton, D. M. *J. Am. Chem. Soc.* **2013**, *135*, 7355-7363.

(39) Waldron, C.; Zhang, Q.; Li, Z.; Nikolaou, V.; Nurumbetov, G.; Godfrey, J.; McHale, R.; Yilmaz, G.; Randev, R. K.; Girault, M.; McEwan, K.; Haddleton, D. M.; Droesbeke, M.; Haddleton, A. J.; Wilson, P.; Simula, A.; Collins, J.; Lloyd, D. J.; Burns, J. A.; Summers, C.; Houben, C.; Anastasaki, A.; Li, M.; Becer, C. R.; Kiviaho, J. K.; Risangud, N. *Polym. Chem.* **2014**, *5*, 57-61.

(40) Nguyen, N. H.; Kulis, J.; Sun, H.-J.; Jia, Z.; van Beusekom, B.; Levere, M. E.; Wilson, D. A.; Monteiro, M. J.; Percec, V. *Polym. Chem.* **2013**, *4*, 144-155.

(41) Nguyen, N. H.; Leng, X.; Sun, H.-J.; Percec, V. *J. Polym. Sci., Part A: Polym. Chem.* **2013**, *51*, 3110-3122.
(42) Anastasaki, A.; Haddleton, A. J.; Zhang, Q.; Simula, A.; Droesbeke, M.; Wilson, P.; Haddleton, D. M. *Macromol. Rapid Commun.* **2014**, *35*, 965-970.
(43) Rosen, B. M.; Jiang, X.; Wilson, C. J.; Nguyen, N. H.; Monteiro, M. J.; Percec, V. *J. Polym. Sci., Part A: Polym. Chem.* **2009**, *47*, 5606-5628.
(44) Nguyen, N. H.; Levere, M. E.; Percec, V. *J. Polym. Sci., Part A: Polym. Chem.* **2012**, *50*, 35-46.
(45) Rosen, B. M.; Percec, V. *J. Polym. Sci., Part A: Polym. Chem.* **2007**, *45*, 4950-4964.
(46) Levere, M. E.; Nguyen, N. H.; Leng, X.; Percec, V. *Polym. Chem.* **2013**, *4*, 1635-1647.
(47) Nguyen, N. H.; Rosen, B. M.; Jiang, X.; Fleischmann, S.; Percec, V. *J. Polym. Sci., Part A: Polym. Chem.* **2009**, *47*, 5577-5590.
(48) Lligadas, G.; Percec, V. *J. Polym. Sci., Part A: Polym. Chem.* **2008**, *46*, 2745-2754.
(49) Lligadas, G.; Rosen, B. M.; Monteiro, M. J.; Percec, V. *Macromolecules* **2008**, *41*, 8360-8364.
(50) Nguyen, N. H.; Levere, M. E.; Kulis, J.; Monteiro, M. J.; Percec, V. *Macromolecules* **2012**, *45*, 4606-4622.
(51) Jiang, X.; Rosen, B. M.; Percec, V. *J. Polym. Sci., Part A: Polym. Chem.* **2010**, *48*, 2716-2721.
(52) Samanta, S. R.; Anastasaki, A.; Waldron, C.; Haddleton, D. M.; Percec, V. *Polym. Chem.* **2013**, *4*, 5563-5569.
(53) Samanta, S. R.; Anastasaki, A.; Waldron, C.; Haddleton, D. M.; Percec, V. *Polym. Chem.* **2013**, *4*, 5555-5562.
(54) Samanta, S. R.; Levere, M. E.; Percec, V. *Polym. Chem.* **2013**, *4*, 3212-3224.
(55) Jiang, X.; Fleischmann, S.; Nguyen, N. H.; Rosen, B. M.; Percec, V. *J. Polym. Sci., Part A: Polym. Chem.* **2009**, *47*, 5591-5605.
(56) Zhang, Q.; Li, Z.; Wilson, P.; Haddleton, D. M. *Chem. Commun.* **2013**, *49*, 6608-6610.
(57) Samanta, S. R.; Cai, R.; Percec, V. *J. Polym. Sci., Part A: Polym. Chem.* **2015**, *53*, 294–303.
(58) Lligadas, G.; Rosen, B. M.; Bell, C. A.; Monteiro, M. J.; Percec, V. *Macromolecules* **2008**, *41*, 8365-8371.
(59) Nguyen, N. H.; Percec, V. *J. Polym. Sci., Part A: Polym. Chem.* **2010**, *48*, 5109-5119.
(60) Nguyen, N. H.; Percec, V. *J. Polym. Sci., Part A: Polym. Chem.* **2011**, *49*, 4241-4252.
(61) Nguyen, N. H.; Sun, H.-J.; Levere, M. E.; Fleischmann, S.; Percec, V. *Polym. Chem.* **2013**, *4*, 1328-1332.
(62) Samanta, S. R.; Sun, H.-J.; Anastasaki, A.; Haddleton, D. M.; Percec, V. *Polym. Chem.* **2014**, *5*, 89-95.
(63) Burns, J. A.; Houben, C.; Anastasaki, A.; Waldron, C.; Lapkin, A. A.; Haddleton, D. M. *Polym. Chem.* **2013**, *4*, 4809-4813.
(64) Chan, N.; Cunningham, M. F.; Hutchinson, R. A. *J. Polym. Sci., Part A: Polym. Chem.* **2013**, *51*, 3081-3096.
(65) Rosen, B. M.; Percec, V. *J. Polym. Sci., Part A: Polym. Chem.* **2008**, *46*, 5663-5697.
(66) Nguyen, N. H.; Rosen, B. M.; Percec, V. *J. Polym. Sci., Part A: Polym. Chem.* **2011**, *49*, 1235-1247.
(67) Levere, M. E.; Nguyen, N. H.; Percec, V. *Macromolecules* **2012**, *45*, 8267-8274.
(68) Guliashvili, T.; Percec, V. *J. Polym. Sci., Part A: Polym. Chem.* **2007**, *45*, 1607-1618.
(69) Grigoras, C.; Percec, V. *J. Polym. Sci., Part A: Polym. Chem.* **2005**, *43*, 319-330.
(70) Percec, V.; Grigoras, C. *J. Polym. Sci., Part A: Polym. Chem.* **2005**, *43*, 5283-5299.

(71) Boyer, C.; Zetterlund, P. B.; Whittaker, M. R. *J. Polym. Sci., Part A: Polym. Chem.* **2014**, *52*, 2083-2098.
(72) Anastasaki, A.; Waldron, C.; Wilson, P.; Boyer, C.; Zetterlund, P. B.; Whittaker, M. R.; Haddleton, D. *ACS Macro Lett.* **2013**, *2*, 896-900.
(73) Soeriyadi, A. H.; Boyer, C.; Nyström, F.; Zetterlund, P. B.; Whittaker, M. R. *J. Am. Chem. Soc.* **2011**, *133*, 11128-11131.
(74) Boyer, C.; Soeriyadi, A. H.; Zetterlund, P. B.; Whittaker, M. R. *Macromolecules* **2011**, *44*, 8028-8033.
(75) Nystroem, F.; Soeriyadi, A. H.; Boyer, C.; Zetterlund, P. B.; Whittaker, M. R. *J. Polym. Sci., Part A: Polym. Chem.* **2011**, *49*, 5313-5321.
(76) Boyer, C.; Derveaux, A.; Zetterlund, P. B.; Whittaker, M. R. *Polym. Chem.* **2012**, *3*, 117-123.
(77) Rosen, B. M.; Lligadas, G.; Hahn, C.; Percec, V. *J. Polym. Sci., Part A: Polym. Chem.* **2009**, *47*, 3940-3948.
(78) Rosen, B. M.; Lligadas, G.; Hahn, C.; Percec, V. *J. Polym. Sci., Part A: Polym. Chem.* **2009**, *47*, 3931-3939.
(79) Percec, V.; Barboiu, B.; Grigoras, C.; Bera, T. K. *J. Am. Chem. Soc.* **2003**, *125*, 6503-6516.
(80) Percec, V.; Grigoras, C.; Kim, H.-J. *J. Polym. Sci., Part A: Polym. Chem.* **2004**, *42*, 505-513.
(81) Percec, V.; Grigoras, C.; Bera, T. K.; Barboiu, B.; Bissel, P. *J. Polym. Sci., Part A: Polym. Chem.* **2005**, *43*, 4894-4906.
(82) Luther, R. *Z. Phys. Chem.* **1901**, *36*, 385-404.
(83) Fenwick, F. *J. Am. Chem. Soc.* **1926**, *48*, 860-870.
(84) Tindall, G. W.; Bruckenstein, S. *Anal. Chem.* **1968**, *40*, 1402-1404.
(85) Ciavatta, L.; Ferri, D.; Palombari, R. *J. Inorg. Nucl. Chem.* **1980**, *42*, 593-598.
(86) Solari, E.; Latronico, M.; Blech, P.; Floriani, C.; Chiesi-Villa, A.; Rizzoli, C. *Inorg. Chem.* **1996**, *35*, 4526-4528.
(87) Hataway, B. J.: Comprehensive Coordination Chemistry; Wikinson, G.; Gillard, R. B.; McCleverty, J. A., Eds.; Pergamon: Oxford, U.K., 1987; Vol. 5, pp 533–774., 1987.
(88) Shriver, D.; Atkins, P.: Inorganic Chemistry, 3rd ed.; Freeman: New York, 1999; pp 195–196.
(89) Wu, S.-H.; Chen, D.-H. *J. Colloid Interface Sci.* **2004**, *273*, 165-169.
(90) Timms, P. L. *Chem. Commun.* **1968**, 1525-&.
(91) Timms, P. L. *Adv. Inorg. Chem. Radiochem.* **1972**, *14*, 121–171.
(92) Negrel, J. C.; Gony, M.; Chanon, M.; Lai, R. *Inorg. Chim. Acta* **1993**, *207*, 59-63.
(93) Wang, W.; Shi, X.; Wang, S.; Van Hove, M. A.; Lin, N. *J. Am. Chem. Soc.* **2011**, *133*, 13264-13267.
(94) Zhang, N.; Samanta, S. R.; Rosen, B. M.; Percec, V. *Chem. Rev.* **2014**, *114*, 5848–5958.
(95) Coca, S.; Jasieczek, C. B.; Beers, K. L.; Matyjaszewski, K. *J. Polym. Sci.: Part A: Polym. Chem.* **1998**, *36*, 1417-1424.
(96) Boyer, C.; Soeriyadi, A. H.; Roth, P. J.; Whittaker, M. R.; Davis, T. P. *Chem. Commun.* **2011**, *47*, 1318-1320.
(97) Fischer, H. *Macromolecules* **1997**, *30*, 5666-5672.
(98) Ganachaud, F.; Balic, R.; Monteiro, M. J.; Gilbert, R. G. *Macromolecules* **2000**, *33*, 8589-8596.
(99) Winstein, S.; Allred, E.; Heck, R.; Glick, R. *Tetrahedron* **1958**, *3*, 1-13.
(100) Allred, E. L.; Winstein, S. *J. Am. Chem. Soc.* **1967**, *89*, 3991-3997.

(101) Zussman, M. P.; Tirrell, D. A. *Macromolecules* **1981**, *14*, 1148-1153.
(102) Shih, J. S.; Tirrell, D. A. *Chem. Eng. Commun.* **1984**, *30*, 219-228.
(103) Percec, V.; Shaffer, T. D.; Nava, H. *J. Polym. Sci., Part A: Polym. Chem.* **1984**, *22*, 637-647.
(104) Shaffer, T. D.; Percec, V. *J. Polym. Sci., Part A: Polym. Chem.* **1986**, *24*, 451-467.
(105) Hajek, M.; Malek, J. *Synthesis* **1977**, 454-457.
(106) Hajek, M.; Malek, J. *Synthesis* **1976**, 315-318.
(107) Lallemand, J. Y. *Tetrahedron Lett.* **1975**, 1217-1218.
(108) Heiba, E.-A. I.; Dessau, R. M. *J. Amer. Chem. Soc.* **1971**, *93*, 524-527.
(109) Hajek, M.; Malek, J. *Collect. Czech. Chem. Commun.* **1977**, *42*, 2388-2393.
(110) Imoto, M.; Ouchi, T. *J. Macromol. Sci.-Rev. Macromol. Chem. Phys. C* **1982**, *22*, 261-302.
(111) Imoto, M.; Ouchi, T. *J. Macromol. Sci.-Rev. Macromol. Chem. Phys. C* **1983**, *23*, 247-316.
(112) Shih, J. S.; Brandt, J. F.; Zussman, M. P.; Tirrell, D. A. *J. Polym. Sci., Part A: Polym. Chem.* **1982**, *20*, 2839-2849.
(113) Wang, X. S.; Armes, S. P. *Macromolecules* **2000**, *33*, 6640-6647.
(114) Ciampolini, M.; Nardi, N. *Inorg. Chem.* **1966**, *5*, 41-44.

**One Sentence, of Maximum 20 words, Highlighting the Novelty of the Work**

Ultrafast, inversely temperature dependent aqueous SET-LRP with "*in situ*" generated Cu(0) yields quantitative chain-ends demonstrating surface mediated activation and termination. (20 words)

**Graphical Abstract**